IMPACT OF ZIKA VIRUS ON HUMAN DENDRITIC CELLS

by

Matthew Good

BS, Shippensburg University of Pennsylvania, 2013

Submitted to the Graduate Faculty of the

Department of Infectious Diseases and Microbiology

Graduate School of Public Health in partial fulfillment

of the requirements for the degree of

Master of Science

University of Pittsburgh

2018

UNIVERSITY OF PITTSBURGH

Graduate School of Public Health

This thesis was presented

by

Matthew Good

It was defended on

April 20, 2018

and approved by

Thesis Director:
Robbie B Mailliard, PhD
Assistant Professor, Infectious Diseases and Microbiology
Graduate School of Public Health
University of Pittsburgh

Committee Member:
Paolo Piazza, PhD
Infectious Diseases and Microbiology
Research Assistant Professor, Graduate School of Public Health
University of Pittsburgh

Committee Member:
Jennifer Adibi, ScD
Assistant Professor, Epidemiology
Assistant Professor, Department of Obstetrics/Gynecology and Reproductive Sciences
Graduate School of Public Health and School of Medicine
University of Pittsburgh

Robbie B Mailliard, PhD

IMPACT OF ZIKA VIRUS ON HUMAN DENDRITIC CELLS

Matthew Good, MS

University of Pittsburgh, 2018

ABSTRACT

Zika virus (ZIKV) is a mosquito-borne flavivirus, transmitted to humans by *Aedes aegypti* and *Aedes albopictus* mosquitos, and has also more recently been shown to transmit from human-to-human sexually and vertically from mother to fetus. ZIKV infection, typically causing mild clinical symptoms, has been linked to a range of neurological complications including microcephaly in fetuses and Guillain-Barré syndrome in adults. ZIKV's recent emergence poses a public health emergency, and new pathological information is required for developing effective interventions to ameliorate the burden of disease. The dendritic cell (DC), the key innate immune responder that ultimately drives anti-viral adaptive immunity, has known interactions with ZIKV. However, the nature of this interaction, and the DCs role in ZIKV pathology needs further elucidation. Here we hypothesize ZIKV can infect and modify the phenotype and function of dendritic cells, which influences the nature of their subsequent interplay with pre-existing ZIKV antigen responsive memory T cells. We found that ZIKV can indeed infect both immature and mature DCs, and that DCs can transfer infection to bystander cells. We also found that exposure of DCs to ZIKV alters their function, maturation status, and survival. Interestingly, we note that the capacity of ZIKV to infect DCs is greatly influenced by the environmental signals received by DCs during their maturation process, and that type-1 polarized DC are inherently more resistant than type-2 matured DC. Importantly, when activated by the $CD4^+$ T

cell helper signal CD40L, ZIKV infected DC proved to be more resistant to ZIKV-induced cell death. And finally, on the background of dengue virus immunity, we found that dengue antigen specific memory T cells cross-react with ZIKV antigen presented by DC, leading to enhanced DC activation rather than elimination. In terms of public health significance, these findings may contribute to our understanding of basic ZIKV and DC interactions, and may help to provide a better understanding of ZIKV pathogenesis leading towards the development of effective interventions to protect and treat those who may become exposed to ZIKV.

TABLE OF CONTENTS

LIST OF FIGURES

PREFACE

Thank you to my advisor, Robbie Mailliard, for taking me onto his team and always giving me the tools and guidance to succeed. Paolo Piazza for your technical knowledge and guidance. Jennifer Adibi for helping bring my work into context and keeping public health a focal point. Thank you to CuraZika. Lastly, a special thank you to everyone in the IDM Lab Group who helped me along the way.

1.0 INTRODUCTION

1.1 OVERVIEW

Zika virus (ZIKV) is a mosquito-borne flavivirus, transmitted to humans by *Aedes aegypti* and *Aedes albopictus* mosquitos but has recently been shown to transmit sexually from human-to-human and vertically from mother to fetus (1, 2). ZIKV infection, typically inapparent or causing mild clinical symptoms, has been linked to a range of neurological complications including microcephaly in fetuses and Guillain-Barré syndrome in adults (3). These adverse complications are increasingly observed in regions endemic for related flavivirus, dengue virus (DENV). ZIKV's recent global outbreaks pose a public health emergency, and new pathological information is required for developing effective interventions to ameliorate the burden of disease.

1.2 ZIKA VIRUS

1.2.1 ZIKV genome and structure

Zika is an enveloped icosahedral virus with a virion size of about 40nm in diameter (projections measuring 5-10nm). Its genome is a positive single-stranded RNA which mimics host mRNA

and has one open reading frame that can directly be translated into a single polyprotein (1, 4). This polyprotein is then cleaved by host and viral proteases into individual viral proteins; 7 structural proteins, C, PrM, and envelope (E), and 7 non-structural proteins, NS1, NS2a, NS2b, NS3, NS4a, NS4b, and NS5 (1, 4). C protein forms the viral nucleocapsid, prM is a precursor to M protein, and E protein is the spike glycoprotein (4). ZIKV E protein is the main target for neutralizing antibodies produced in response to infection.

1.2.2 Binding and Life Cycle

Like all flaviviruses, ZIKV attaches to host cells by binding of viral E proteins to glycosaminoglycans (GAGs) on the surface of cells (3). Viral E protein, which is N-glycosylated, can also interact with the dendritic cell-specific intercellular adhesion molecule-3-grabbing non-integrin (DC-SIGN) on the cell surface (3). DC-SIGN is found on a variety of cell types including DCs and macrophages (4). Cellular lectins and TIM and TAM families of receptors have also been implicated in flavivirus attachment to cells. Cell entry is subsequently completed by clathrin-dependent endocytosis and membrane fusion (3). Ph-dependent fusion in endosomes then occurs and viral RNA is released into cell cytoplasm. Viral RNA can be directly translated in the endoplasmic reticulum followed by particle assembly, maturation, and release from the cell (4).

1.2.3 Tissue Tropism

Cell types known to be permissive to ZIKV include immature dendritic cells (DC), dermal fibroblasts, epidermal keratinocytes, endothelial cells, placental macrophages called Hofbauer

Cells (HC), placental cytotrophoblasts, and placental trophoblasts (5, 6). Multiple genotypes of ZIKV exist, but evidence suggests there is only one serotype, and immune responses appear to be cross-protective between genotypes (7). However, the risks of adverse neurological outcomes do appear to differ by genotype.

1.2.4 ZIKV Distribution and Current Treatments

ZIKV was first isolated in 1957 in Uganda but has since spread to regions around the globe. Zika is currently found in Africa, Asia, The Caribbean, Central America, North America, the Pacific Islands, and South America (8). Two primary lineages of ZIKV can be traced-African and Asian (4, 7). These lineages share greater than 95 percent amino acid sequence identity.

Outbreaks of ZIKV occurred in French Polynesia in 2013 and were followed by a significant ZIKV emergence in Brazil in 2015, bringing renewed attention to the virus (9). Soon after, the virus spread to the rest of the Americas (9, 10). General increases in the prevalence of ZIKV still are being observed, despite a slight recent decline over the most recent year. ZIKV infections in the Americas in the last 3 years have reached 230,000 cases and this includes 222,986 autochthonous and 6252 imported cases (11, 12). Along with the increase in the prevalence of ZIKV infection, increases in the prevalence of congenital ZIKV syndrome and associated neurological complications have been observed.

There are no licensed antivirals or vaccines currently approved for the treatment of ZIKV, but several vaccines are in development and clinical trials (13, 14).

1.2.5 Clinical ZIKV

Acute ZIKV infection is typically inapparent, with 80% infected individuals showing no symptoms, while an estimated 20% of patients display a variety of self-limiting clinical presentations including rash, fever, fatigue, and other minor symptoms that rarely result in hospitalization (15). Despite typically causing mild disease, ZIKV has been linked to a range of neurological diseases, including Guillain-Barré, acute disseminated encephalomyelitis (ADEM), optic neuritis, meningoencephalitis and acute myelitis (9, 16). Congenital Zika syndrome has recently become of large concern. Vertical transmission from mother to fetus has been observed and fetal infection can lead to a range of neurological and developmental complications in newborns including microcephaly, primitive reflexes, tremors/convulsions, calcifications, and others (9, 17). These symptoms can also be found in infants with normal skull diameter (17).

1.3 ZIKV AND DENDRITIC CELLS

The DCs are known to be targets of infection for other flaviviruses including, dengue virus (DENV), West Nile virus (WNV), yellow fever virus (YFV) and Japanese encephalitis virus (JEV) (18). Despite known circumstances surrounding these flaviviruses, there is a major gap in the knowledge of the role that the DC plays in ZIKV pathogenesis as well as ZIKVs general impact on DCs. DCs form the link between innate and adaptive immune responses. During the early stages of infection, DCs are initial responders and become activated and programmed by their environment to guide the subsequent the immune response. They next assume a regulatory role by migrating to lymph nodes and priming antigen specific T cells. The effector phase of the

immune response follows this, which is critical for mounting a successful response to a pathogen and development of memory responses. The DC is likely a critical cell type during ZIKV infection, and modulations in the normal function of the DC or alterations to the microenvironment of the DC in which they are programmed in early infection, may contribute to the disease state: pathogenic outcome vs successful immune response.

A previous report by Bowen et al. indicated that ZIKV can productively infect immature DCs and that ZIKV 'slightly' alters the DC phenotype and profile of pro-inflammatory cytokine secretion (18). There is considerable variability in replication and downstream effects on DCs between different donors as well as between different ZIKV strains (18). Viral binding between donors appears to be similar indicating any differences in replication or downstream effects most likely are a component of variation in cell processes donor to donor (18). Despite these findings, a different group (Sun et al.) recently reported data contradictory to these in vitro findings (18, 19). Bowen et al., report minimal upregulation of T cell co-stimulatory molecules and MHC molecules in *in vitro* infection, while Sun et al. 2017 reports co-stimulatory molecules and activation markers were downregulated in *in vitro* infection (18, 19). The reason for these different *in vitro* findings is not clear and highlights the need to further explore ZIKV impact on DC.

It is critical to determine the true outcome of DC infection with ZIKV on type I interferon (IFN) responses, due to the role interferons play in driving anti-viral responses. Bowen et al., additionally showed RIG-I, a dsRNA pattern recognition receptor, agonist treatment potently restricting ZIKV replication while type I IFN treatment had minimal effects on restricting ZIKV replication (18). Other recent reports suggest ZIKV could target STAT1 and STAT2, signal transducing factors involved in mediation of immune signaling (20, 21). The consensus is that

ZIKV can inhibit normal interferon responses to antigen type I IFN signaling. RIG-I and type I IFN responses are critical for inducing the antiviral response to flaviviruses (2). If IFN genes are systematically downregulated, as some reports suggest, this will lower intrinsic antiviral activity and the priming of adaptive responses (19).

Cell survival in DCs following ZIKV infection has not been explored in detail. ZIKV is known to induce apoptotic cell death in neuronal cells, and triggers cell death of surrounding neurons, but how or if these neurotoxic mechanisms apply in the context of other cells or in relevant microenvironments is unknown (22).

Despite these recent findings, somewhat misleading and contradictory reports, and general lack of DCs known role in pathogenesis, more information is required to fully understand ZIKVs impact on DC function and survival. The goal of this project was to expand the knowledge relating to the role of the DC in ZIKV pathogenesis.

1.4 OTHER FLAVIVIRUSES

Other prominent members of the flavivirus family include DENV, West Nile virus (WNV), Yellow Fever virus (YFV) and Japanese encephalitis virus (JEV). This genus is characterized by similarities in genomes, pathogenesis, methods of transmission (1). Unlike ZIKV, DENV has 4 known serotypes (DENV-1, DENV-2, DENV-3, and DENV-4), and these serotypes present different clinical outcomes and research challenges. Dengue hemorrhagic fever (DHF), a severe form of dengue fever, may occur when an individual with existing immunity to one serotype becomes infected with a different serotype. The leading hypothesis for this phenomenon is called antibody-dependent enhancement (ADE); sub-neutralizing, cross-reactive antibodies facilitate

increased viral load and inflammation leading to severe disease (23). While it is known that cross-reactive antibody responses can contribute to DHF, current evidence suggests both the possibility of protective and dysfunctional roles that DENV memory T cells could play in pathogenesis (8, 23, 24).

1.4.1 Zika and Dengue Virus

DENV memory cell cross-reactivity becomes important in the context of ZIKV. ZIKV has emerged in regions hyper-endemic for DENV, raising the chances that ZIKV could infect an individuals with pre-immunity to DENV, and ZIKV / DENV show sequence homology up to 68% for more highly conserved proteins (24). Knowing this similarity, whether DENV memory T cells would respond to ZIKV antigen during ZIKV infection, is unknown. Studies of lymphocytic choriomeningitis virus in mice indicated cross-reactive T cells could result in either normal protective responses or altered viral pathogenesis (25). Our group reported in HIV that $CD8^+$ effector memory T cells recognizing HIV escape variants lead to the absence of killing of the target and promote viral dissemination and persistence (26). If cross-reactive DENV memory T cell populations exist, their interaction with DC presenting ZIKV antigen could lead to similar outcomes. It is possible that cross-reactive T cells could lead to a swift and effective immune response or they could enhance ZIKV pathogenesis. Specifically, atypical effector memory cell responses could impact normal antigen-presenting function of DCs, affect DC activation and maturation, alter cytokine secretion contributing to increase inflammation in tissue microenvironment, or even promote survival of infected DCs leading to dissemination and persistence of ZIKV.

1.5 ZIKA AND THE MATERNAL-FETAL ENVIRONMENT

Viral RNA and infectious virions can be detected in placenta, amniotic cavity, and fetal CNS of babies with microcephaly (17). While ZIKV has recently been shown to transmit human-to-human sexually and vertically from mother to fetus the exact vertical transmission route has not been confirmed. The placenta is a physical and immunologic barrier between the maternal and fetal compartments and many contacts form between the two (2, 27). Several cell types may be involved in transmission of ZIKV if it in fact occurs at the maternal fetal interface. Layers of primary trophoblasts called syncytiotrophoblasts (STB) are in direct contact with maternal blood, but found to be non-permissive to ZIKV infection due to type-III interferon production in these cell types (27). Cytotrophoblasts (CTB), another cell type of chorionic villi that form the layer behind STBs, were shown to support ZIKV infection to an extent (2). Placental macrophages called Hofbauer cells are permissive to ZIKV infection. In the placental-fetal compartment, dendritic cells are primarily resident in the decidua which is an interface between the fetal placenta and the uterus (28). Decidual macrophages are sites of ZIKV infection (28); however decidual dendritic cells have not been studied in the context ZIKV infection. Our findings here, using human myeloid derived DC, may help us speculate if the decidual DC could be implicated in ZIKV maternal fetal transmission.

2.0 STATEMENT OF THE PROJECT

ZIKV's impact on DCs and their role in ZIKV pathogenesis remains loosely defined, and therefore must be further explored. In addition, the responses of T cells to ZIKV presenting DC, the existence of cross-reactive T cell responses to ZIKV antigen presenting DC, and the mechanisms of vertical transmission that result in congenital ZIKV are still not fully understood. New neurological manifestations are being defined and the capacity of future outbreaks of ZIKV and associated congenital disease are unknown. This highlights the urgency to extend knowledge of ZIKV pathogenesis. Any new knowledge pertaining to the following aims will potentially drive the development of potential treatments, prevention of maternal/fetal transmission, or lead to the production of more effective vaccines that exploit ZIKV-specific dendritic cell responses. This project was made possible by collaborations between Pitt Public Health and FIOCRUZ and funding from CuraZika Alliance.

3.0 SPECIFIC AIMS

3.1 AIM 1

Aim 1: Assess the direct impact of ZIKV on the phenotype and function of dendritic cells

Aim 1 focuses on modeling the specific events that follow the initial exposure of DC to ZIKV. The primary objective to model these events involves the direct impact of ZIKV on the phenotype and the function of DCs.

The following questions will be approached:

- Can DC be infected?
- How does DC exposure to ZIKV impact DC maturation/activation?
- Does ZIKV affect DC survival?
- Does ZIKV impact DC cytokine production?
- Does the maturation/polarization status of the DC affect their capacity to be infected?
- Can infected DC produce infectious virus and disseminate ZIKV to other cells?

3.2 AIM 2

AIM 2: Model interactions of ZIKV antigen-presenting dendritic cells with DENV memory T cells

Aim 2 focuses on the context of the T cell interaction with APCs following ZIKV infection. The survival and downstream dynamics of ZIKV exposed DC in response to T cell signals will be assessed, as well as how this may alter the cellular microenvironment contributing to ZIKV pathogenesis.

3.2.1 Sub-aim 2A

Sub-aim 2A: Explore the impact of the Th signal CD40L on ZIKV infected DC

To determine the impact of T cell help on ZIKV infected DCs, $CD4^+$ T helper (Th) cell surrogate CD40L will be used. The effect on the survival, the persistence of infection, cytokine production and maturation of ZIKV exposed myeloid-derived DC receiving the CD40L T cell helper signal will be determined. A component of this aim entails determining the capacity of productively infected DCs receiving T cell help in mediating ZIKV transfer and infection to other cell types.

- Use CD40L as a surrogate for $CD4^+$Th cell interaction
- Impact on CD40L-induced IL-12p70 production
- DC survival
- Virus production

- Inter-cellular transfer and infection

3.2.2 Sub-aim 2B

Sub-Aim 2B: Determine if ZIKV Ag presenting DC induce cross-reactive responses from heterologous Flavivirus specific memory T cells

Directly characterize T cell responses to ZIKV antigen-loaded autologous DC from participants of a local study cohort who are seropositive for DENV. The presence of cross-reactive T cells in donors with pre-existing immunity to related flavivirus, DENV, will be assessed. The impact of such cross-reactive T cells on driving subsequent immune events and their effect on viral containment, dissemination, or disruption of the microenvironment will be analyzed.

3.3 HYPOTHESIS

Overarching hypothesis:

ZIKV can infect and modify the phenotype and function of dendritic cells (DC), which can impact the nature of their subsequent interplay with pre-existing ZIKV-Ag responsive flavivirus memory T cells.

The result of very early innate responses to ZIKV infection will play a major role in the outcome of the disease; successful elimination of the pathogen vs pathogenic outcome. The result of DCs interaction with ZIKV is most likely critical knowing the importance of DCs in early infection and their critical role linking innate and adaptive immunity. We hypothesize the

impact of ZIKV on the survival and function of DC is a component of the immune response that will contribute to the pathologic conditions of ZIKV infection. ZIKV infected DC receiving T helper signal will promote the enhanced survival of ZIKV infected DCs and contribute to viral persistence, dissemination, altering the immune backdrop and may cause a disruption of tissue microenvironment further enhancing ZIKV pathogenesis based on our knowledge of CD40L effects as a mediator of DC inter-cellular transfer. We hypothesize that ineffective cross-reactive responses from flavivirus specific memory T cells will alter the DC-mediated responses to primary ZIKV infection compounding enhancement of disease state - dysfunctional DC to T cell interactions responses will negatively alter DC-mediated innate and adaptive responses and clearance of ZIKV. The result of exploring this hypothesis will elucidate new details on ZIKV pathogenesis and hopefully a greater picture of the disease state contributing to the maternal-fetal interactions leading to congenital ZIKV

4.0 MATERIALS AND METHODS

4.1 DONOR SAMPLES

Peripheral blood samples from healthy donors were obtained from blood products via Central Blood Bank of Pittsburgh. Cryopreserved peripheral blood mononuclear cells (PBMC) obtained from a previously established Pittsburgh DENV cohort of study participants of known immune status to Flavivirus were also used in this study. The cohort comprised of participants from Central America and South America who were determined to be DENV IgG positive or DENV IgG negative.

4.2 PRIMARY CELL ISOLATION FROM BUFFY COAT

PBMC isolated from blood of DENV seropositive or seronegative donors using ficoll density gradient separation and separated into $CD14^+$ cell subset or peripheral blood lymphocytes followed by cryopreservation. Positively selected $CD14^+$ monocytes and negatively selected $CD14^-$ lymphoctyes were isolated from PBMC using $CD14^+$ MicroBeads, LS column, and MidiMACS^{TM} separator (Mitenyi Biotec). In addition, $CD3^+$, $CD8^+$, $CD4^+$ T cells were isolated using positive or negative selection kits (EasySep, STEMCELL Technologies).

4.3 GENERATION OF HUMAN MONOCYTE-DERIVED DENDRITIC CELLS

Monocytes were cultured at 37°C in a 5.0% CO2 environment for 5 days in Iscove's Modified Dulbecco's Medium (IMDM) (Gibco Laboratories) supplemented with 10% heat inactivated fetal bovine serum (FBS) and 0.5% gentamicin (Gibco Laboratories) with addition of rhIL-4 (2µg/mL) and rhGM-CSF (2µg/mL). This gave rise to $CD14^-$ immature DC (iDC)

4.4 MATURATION OF MONOCYTE-DERIVED DENDRITIC CELL CULTURES

iDC were matured by the addition of activation factors directly into culture wells on day 5 of incubation followed an additional 48h culture period. The resulting differentially matured and polarized DC types were generated using the respective listed set of maturation factors:

DC0: rhCD40L – 1 µL/mL from stock to a final concentration of 0.09 µg/mL, or TNF- α 20 ng/mL

DC1: rhTNF-α (20 ng/ml), rhIL-1β (10 ng/ml), rhIFN-γ 1000 U/mL

αDC1 (specialized DC1 type) rhTNF-α (20 ng/ml), rhIL-1β (10 ng/ml), Poly-I:C (20 µg/ml), rhIFN-α (1000 IU/mL), rhIFN-γ (1000 IU/mL)

DC-2: rhTNF-α (20 ng/ml), rhIL-1β (10 ng/ml), rhIL-6 (10 ng/ml), and PGE-2 (2 µM)

4.5 ZIKV PROPAGATION AND TITRATION

PRVABC59 (PR-2015) strain, isolated in Puerto Rico in 2015, was used in all experiments. PR-2015 propagation was performed in *Aedes albopictus* clone C6/36 cells. Supernatant from C6/36 cells isolated and concentrated using Centricon® plus-70 Centrifugal Filter (Millipore Sigma). Work performed by Dr. Paolo Piazza, who kindly donated virus. Quantification of the virus was performed using Vero cell plaque assay to determine number of plaque forming units (PFU) per unit volume of a virus preparation.

4.6 ESTABLISH C6/36 SUPERNATANT CONTROLS

C6/36 cells supernatant controls prepared using ZIKV propagation methods, in absence of virus. Supernatant controls used in experiments alongside un-infected controls and experimental infected samples.

4.7 GROWTH AND MAINTENANCE OF VERO CELL CULTURES

Vero cell line maintained in RPMI supplemented with 10% FBS, and 2.5% HEPES buffer. Vero cells propagated from frozen stocks, maintained and passaged upon reaching 95% confluence as outlined in Ammerman, 2008 (29).

4.8 ZIKV INFECTION OF CELLS

Immature DC infected at day 5 of culture. DC harvested from wells by gently pipetting up and down followed by a wash with cold 1X PBS. Cells washed and resuspended to determine concentration followed by adjusting to desired concentration. Cells resuspended with 100uL virus inoculum at desired multiplicity of infection (MOI) (MOI of 1 is a ratio of 1cell:1PFU) 37°C 5.0% CO2 for 1-2hrs. Cells resuspended to the desired concentration and distributed to wells of 96-well v-bottom format, or desired well format required by experiment. Condition medium added back to wells and incubated at 37°C 5.0% CO2 for desired length of time.

4.9 FLOW CYTOMETRY

Flow cytometry was used to measure the expression of various surface protein markers on DC (CD80, CD86, CD83, HLA-DR, DC-SIGN, CD14, SIG-1, HLA-ABC). BD LSRFortessa™ cell analyzer was used for all flow cytometry acquisitions and FACS Diva acquisition software. Data analysis and preparation using FlowJo Software (FlowJo, LLC).

4.10 FLAVIVIRUS GROUP ANTIGEN DETECTION

Cells fixed and permeabilized for 20 mins prior to intracellular staining (ISC) using Cytofix/Cytoperm (BD Biosciences) followed by staining with a primary mouse monoclonal anti-4G2 antibody generated in Hybridoma Cell line. Primary followed using IgG2a goat anti-

mouse directly conjugated to PE (Invirogen Cat # P-852). Additionally, directly conjugated Flavivirus group antigen Antibody (D1-4G2-4-15) (Novusbio) used. Cells were fixed in PFA 1% and analyzed BD LSRFortessa™ cell analyzer.

4.11 MSD MULTIPLEX ELISA

Cellular expression of cytokines and chemokines involved in inflammation including IFN-γ, IL-1β, IL-2, IL-4, IL-5, IL-8 (CXCL8), IL-10, IL-12 p70, IL-13, and TNF-α were quantified using Mesoscale Development (MSD) U-PLEX TH1/TH2 Combo kit (MSD Cat# K15071K-1 and K151ACC-1). This panel includes cytokines which are involved in inflammatory responses and that are implicated in the T helper (Th) 1 and Th2 pathways. All manufacture protocols followed, and acquisition performed using MSD platform.

4.12 CELLTITER-GLO® LUMINESCENT CELL VIABILITY ASSAY

Cell-Titer GLO luminescent cell viability assay was used to detect cell death. Reagents were reconstituted as outlined in manufacturer's protocols (Promega Corporation Cat# G7570) and an initial titration of cells was performed to determine optimum number and ensure values were within the linear range of CellTiter Glo. Analysis was performed in 96-well format (opaque plates) in triplicate. Perform serial 2-fold dilution of cells starting from 100,000 cells in 200uL (perform 6, 1:2 dilutions). A volume of reconstituted reagent equal to the volume of cells in wells was added to cells in suspension. Contents mixed and incubated for 2 mins in an orbital

shaker to induce lysis followed by incubation for 10 mins at RT. Luminescence was recorded using Luminometer (Veritas™ Microplate Luminometer, Turner BioSystems). To perform cell viability assay on experimental samples, 100µL cells at $1.0x10^6$ added directly to wells of 96-well format (opaque plates). Samples incubated for desired length of time at 37°C 5.0% CO2 followed by development as described above.

4.13 NONYL ACRIDINE ORANGE MITOCHONDRIAL PROBES

Staining of negatively charged phospholipids in cell mitochondrial membranes using Acridine Orange 10-Nonyl Bromide (NAO) (Invitrogen Cat#A1372) to detect early-stage apoptosis. Stock solution was prepared in 100% ethanol at 50ug/mL. 25ng/mL working stock was prepared on ice in PBS/0.5% BSA. $2.5x10^5$ – $5.0x10^5$ cells in 500µL were added to polystyrene FACS tubes, centrifuged and resuspended in 500µL NAO working stock and then incubated 4°C for 10min. 1mL PBS-BSA added to each tube and centrifuge 550g 5 min. NAO solution removed and resuspend in PBS-BSA or 1.0% PFA for ZIKV infected cultures. Fluoresce analyzed using flow cytometer on FITC channel (Wavelength Maxima: Excitation 495nm, Emission 519nm) (BD LSRFortessa™ cell analyzer).

4.14 MICROSCOPY

Cell imaging was performed using Leica DMIL IL LED (Leica Microsystems) inverted laboratory microscope at 10x, 20x, or 40x magnifications. Images were captured and processed using Leica Application Suite - LAS EZ.

4.15 GENERATION OF FLAVIVIRUS PEPTIDES

Flavivirus NS3 peptide sequences were determined for DENV, ZIKV, and WNV by Dr. Paolo Piazza using publicly available sequences from NCBI. The 18mer peptide antigens derived from these sequences were purchased from Sigma, resuspended in DMSO at a stock concentration of 10 mg/ml and subsequently used to make representative NS3 peptide pools for respective Flaviviruses.

5.0 RESULTS

5.1 AIM 1

5.1.1 Human iDC can be infected with ZIKV

The ability of DCs to be infected as well as to have a reliable means of detecting infection was critical to further examine the role of DC in ZIKV pathogenesis, and to assess the aims outline above. It is has been previously reported that DCs can be infected, however we first set out to test and verify this using the donor cells and ZIKV strains planned for the proposed research. Using flow cytometry, iDC were determined to be infected 48h after their initial 2h exposure to ZIKV and compared alongside reliable uninfected control cells (Figure 1).

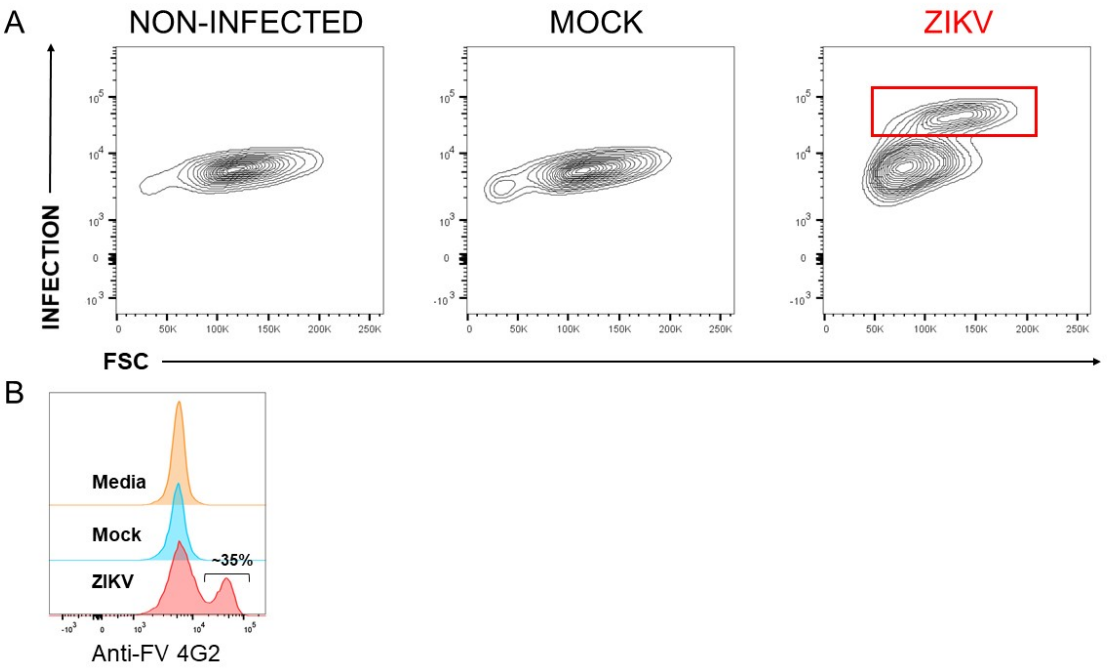

Figure 1 Human iDC can be infected with ZIKV

Monocytes differentiated into iDC using IL-4 and GM-CSF (outlined in Materials and Methods). iDC harvested on day 5 and left non-infected, mock-infected, or infected with ZIKV PR-2015 at a multiplicity of infection (MOI) of 1. Cells harvested and stained for Flavivirus viral E protein 48hrs PI and analyzed using flow cytometry. Figure (A) Flow cytometry FSC vs SSC of controls and ZIKV PR-2015. One representative experimental sample shown. Figure (B) Flow cytometry data showing histogram (normalized to mode) for anti-Flavivirus detection anti-body.

5.1.2 Detecting infection thorough time course infection

The detection method for infection utilizes ICS and direct detection of flavivirus envelope protein within cells. To confirm detection of viral E protein at the experimental time points is not a result of the detection of E protein from virus used in the initial infection, a time course experiment was performed. No viral E protein is detectible at 2 hours post infection (Figure 2). Peak infection (previously shown to be 48 hours) occurs followed by a declining over several days, and this is confirmed using our donors and strains. A standard time point post infection for

analyzing the level of infection was chosen at 48 hours. Differences in the percentage of infection were observed among donors.

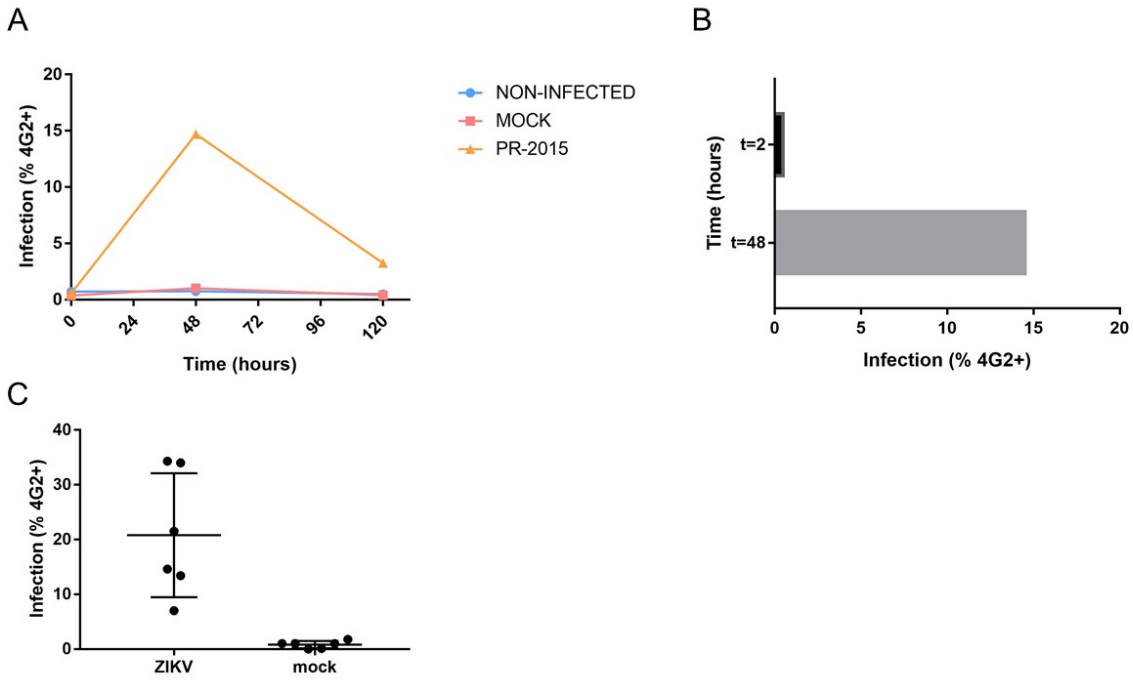

Figure 2 Time course infection and donor variability

Three separate iDC cultures from the same donor were infected at MOI of 5. Cells were washed twice with condition media and let to incubate for either 2 hours, 48 hours, and 120 hours at 37°C, 5% CO2. Cells stained for Flavivirus viral E protein at 2hr, 48hrs, and 120hrs PI and analyzed using flow cytometry. Figure (A) Time course showing total iDC populations infection level detectible via anti-4G2. Figure (B) Bar graph depicting percent total DC infected at 2 vs 48 hours. Figure (C) ZIKV infection variation at 48 hours across experiments. Infected samples vs mock control. Percent infection based on total DC population and plotted on scatter plot with mean standard deviation.

5.1.3 Type I IFN potently restricts ZIKV infection of iDC

Previously published research suggested that ZIKV evades type I interferon responses in vitro, so we explored this by stimulating infected DC with IFN-α, a type I interferon (18). Our positive iDC control indicated DCs were infected at a rate of roughly 50%. But in cultures exposed to IFN-a, infection was almost completely inhibited.

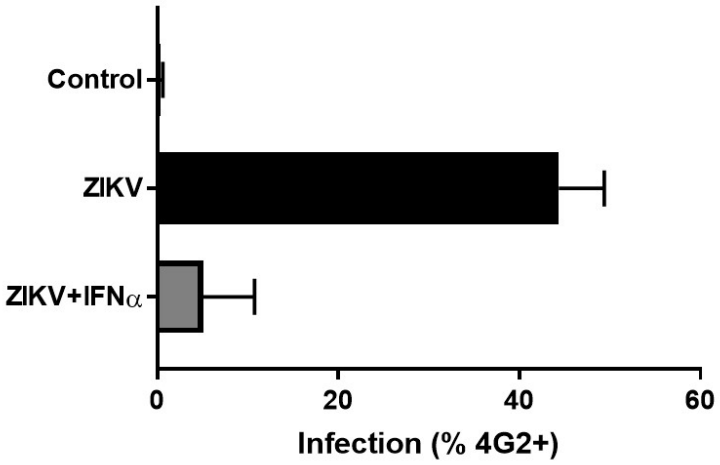

Figure 3 Type one IFN (IFN-α) has capacity to restrict ZIKV in DCs

Monocytes differentiated into iDC using IL-4 and gm-CSF. iDC harvested on day 5 and left non-infected, mock-infected, or infected with ZIKV PR-2015 at a multiplicity of infection (MOI) of 1. Infection control (iDC), non-infected control (mock), and iDC stimulated with IFN-α added directly to culture after infection. Cells stained for Flavivirus viral E protein 48hrs PI and analyzed using flow cytometry. Averages from two donors with error bars representing mean standard deviation.

5.1.4 ZIKV causes modest upregulation of maturation associated protein markers in iDC

Reports regarding the maturation status of iDC upon exposure to infection with ZIKV *in vitro* need clarified. Therefore, we tested the surface expression of various maturation associated markers on iDC 48h post exposure to ZIKV. When comparing total iDC population maturation associated protein markers (CD80, CD86, HLA-DR), a modest up-regulation of all markers tested was determined (Figure 4A-C).

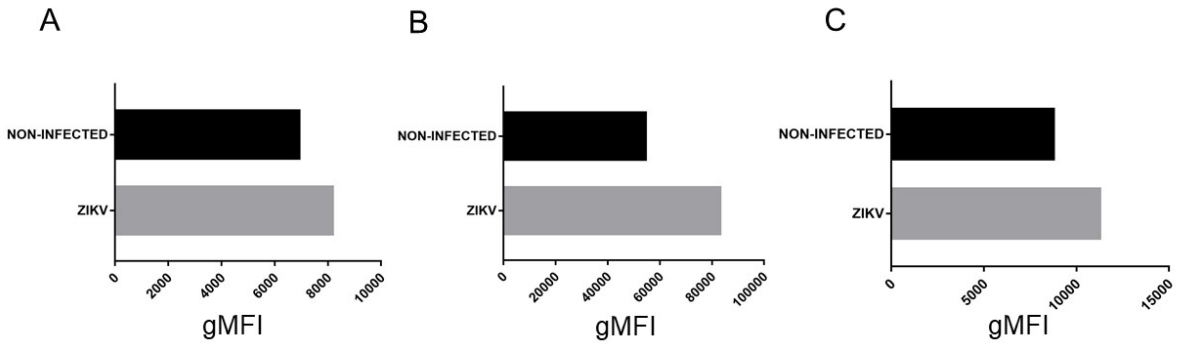

Figure 4 ZIKV upregulates cell surface maturation associated protein markers in iDC

iDCs left non-infected or infected with ZIKV PR-2015. Cells stained for Flavivirus viral E protein 48hrs PI to confirm infection (data not shown). Cells surface stained for maturation associated protein markers CD86, CD80, HLA-DR and analyzed using flow cytometry. Gate on the total iDC population based on forward and side light scatter properties (FSC/SSC). Figure (A), the geometric mean fluorescence intensity of CD80 higher in PR-2015 samples compared to non-infected control. Figure (B), the geometric mean fluorescence intensity of CD86 higher in PR-2015 samples compared to non-infected control. Figure (C), the geometric mean fluorescence intensity of HLA-DR higher in PR-2015 samples compared to non-infected control.

5.1.5 ZIKV Exposure inducing morphologic DC changes

An unexpected observation was the formation of two populations in iDC cultures exposed to ZIKV. When ZIKV culture compared to mock (Figure 5A) there is a large shift in the cell population to a lower FSC. This effect was explored further in more donors. Mean size, as a component of FSC, was found to be about 20% lower in ZIKV exposed cultures at 48hr PI (Figure 5B).

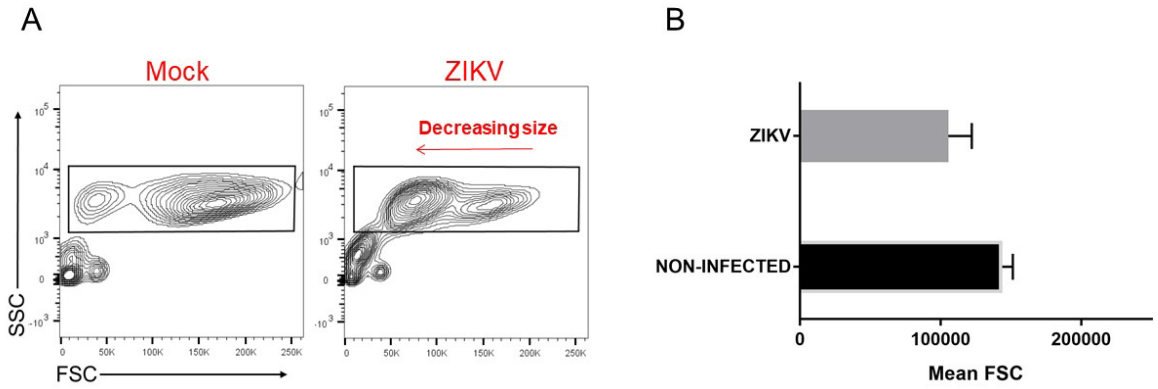

Figure 5 ZIKV infection causes morphologic changes in iDCs

iDCs were infected with PR-2015. Cells stained for Flavivirus viral E protein 48hrs PI and analyzed using flow cytometry. Figure (A) shows flow cytometry FSC vs SSC comparing the mock control and ZIKV exposed cultures. Figure (B) Average geometric mean FSC intensity of total DC population between two donors. Gated on total DC populations, error bars representing mean standard deviation. Samples infected with ZIKV PR-2015 display decreased mean FSC.

5.1.6 The larger DC subset (FSC high) shows highest evidence for ZIKV infection

To further explore the observed morphological changes occurring in the ZIKV exposed cultures (Figure 5), a more detailed analysis was performed. Gating strategy was changed to encompass the smaller (FSC low) and larger (FSH High) cell populations in ZIKV culture (Figure 6A). In these populations infection rates were then determined. The larger cell population showed to be 60% infected while the smaller population was only 16% infected (Figure 6B).

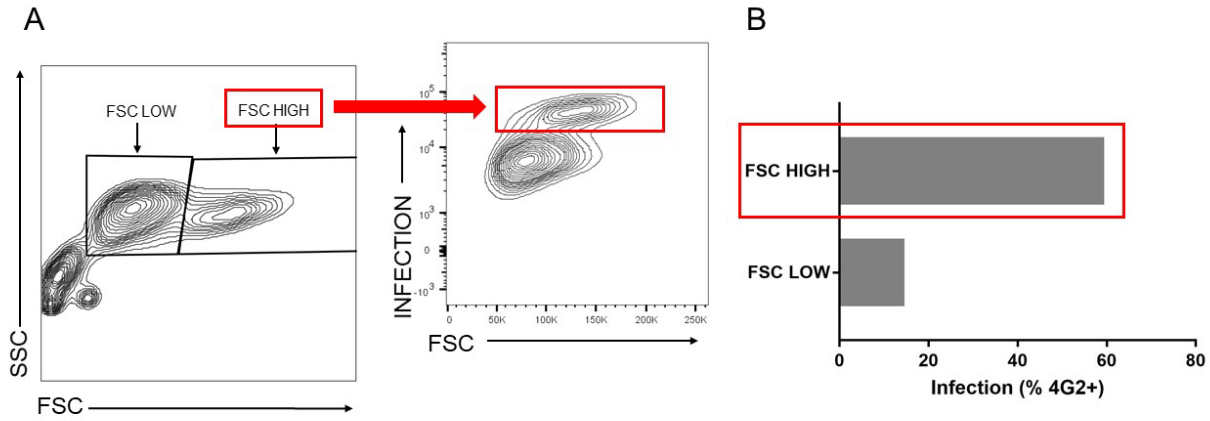

Figure 6 Measurable ZIKV infection is limited DC that are larger

iDC harvested on day 5 and left non-infected, mock-infected, or infected with PR-2015 (infected samples shown only). Cells stained for Flavivirus viral E protein 48hrs PI and analyzed using flow cytometry. Figure (A) Gating on small (FSC low) and larger (FSC high) subsets of DC. The second panel shows FSC vs anti-4G2 compared showing the shape of the larger population being more infected. Figure (B) Comparison of percent infection between the two subsets in figure A.

5.1.7 ZIKV Infected DC subset have higher expression of maturation markers

The same gating strategy shown in Figure 6 was used to explore the expression of maturation associated protein markers in the smaller and larger DC populations. Maturation associated markers CD80, CD86, and HLA-DR are expressed at moderately higher levels (based on MFI) in the larger cell populations compared to the smaller cell population.

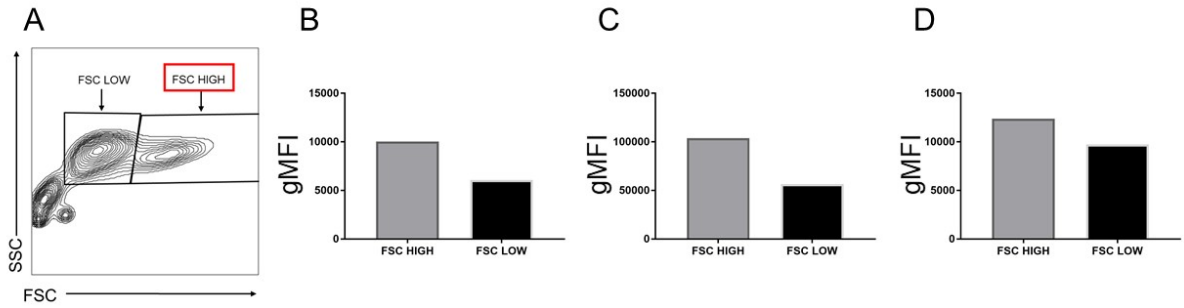

Figure 7 Measurable ZIKV infection is limited DC more mature phenotypically

iDC Harvested on day 5 and left non-infected, mock-infected, or infected with PR-2015 (infected samples shown only). Cells surface stained for maturation associated protein markers CD86, CD80, HLA-DR and analyzed using flow cytometry. Figure (A) FSC by SSC analysis showing the large and small populations. Figure (B) geometric mean fluorescence intensity of CD80 higher in FSC HIGH samples compared to FSC LOW. Figure (C) geometric mean fluorescence intensity of CD86 higher in FSC HIGH samples compared to FSC LOW. Figure (D) geometric mean fluorescence intensity of HLA-DR higher in FSC HIGH samples compared to FSC LOW

5.1.8 Are the ZIKV-induced changes in iDC size indicative of apoptosis?

The observed changes in Figure 5 raise the question if the shrinking occurring is apoptosis. Shrinking and blebbing of cells is known hallmark of apoptosis. To show that this pattern indeed occurs when cells are experiencing apoptotic death, UV radiation was used to replicate this pattern. UV radiation induces apoptotic cell death. A comparable shrinking pattern is indeed observed when we exposed iDC to UV radiation (Figure 8A). Using a cell viability dye, total DC

viability of non-infected control was compared to cells exposed to ZIKV virus. Minimal differences observed between control and ZIKV exposed groups using LIVE/DEAD labeling.

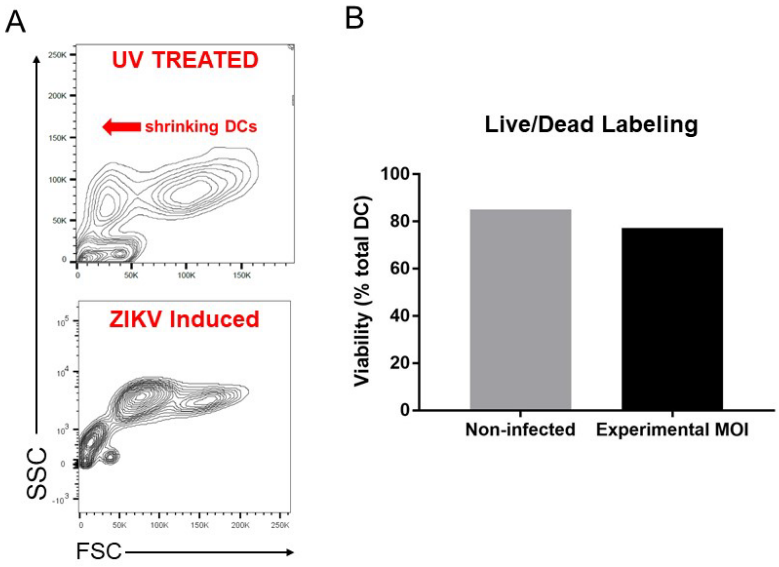

Figure 8 Is ZIKV induced shrinkage indicative of DC apoptosis?

Figure (A) DC were treated with short term exposure to UV light and analyzed using flow cytometry 48h post treatment (Upper panel, non-UV exposed not shown) and compared to ZIKV induced shrinking (Lower panel) Figure (B) The viability of total DC population determined using live/dead labeling. Non-infected control compared to cells exposed to MOI of virus that is typical in experiments.

Structure and integrity of mitochondria were assessed using 10-N-nonyl-acridine orange (NAO). In cultures exposed to ZIKV, increases in early apoptotic events were detected at higher percentages compared to the mock control (Figure 9A). The apoptotic cells, determined through loss of ability to retain NAO probe, are indeed smaller in size compared to non-apoptotic cells (Figure 9B).

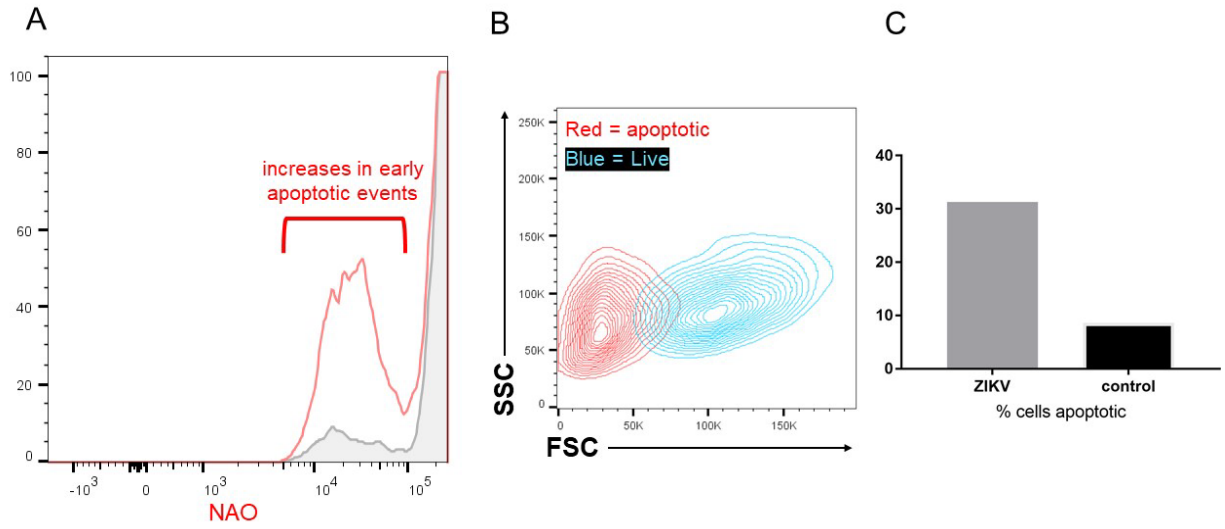

Figure 9 Exposure to ZIKV results in iDC apoptosis (as determined by nonyl acridine orange staining

Structure and integrity of mitochondria are assessed using 10-N-nonyl-acridine orange (NAO). Staining of negatively charged phospholipids in cell mitochondrial membranes allows for detection of apoptosis. Harvested on day 5 and left non-infected, mock-infected, or infected with PR-2015. Cells stained for Flavivirus viral E protein 48hrs PI to confirm infection (not shown) and analyzed using flow cytometry. Figure (A) Histogram showing the intensity of NAO staining. ZIKV treated group (shown in RED) has a larger percentage of cells where mitochondria have lost the capacity to stain positive for NAO. Normalized to mode, unstained control not shown. Figure (B) FFC by SSC showing the size of cells with capacity to stain positive for NAO, and cells losing ability to retain stain as they become smaller (decrease in FSC). Red contour plots represent the light scatter properties of the NAO dim stained cells gated in panel A and the rest of the NAO high DCs shown in blue. Figure (C) Percent of cells apoptotic based on NAO staining shown between ZIKV and control cultures.

To further explore cell death, cell was viability examined using an assay to assess metabolic activity by quantitating cellular ATP levels present in cultures. In all donors, ZIKV exposed cultures showed reduced ATP at 48 hours post infection compared to non-infected and mock infected controls (Figure 10).

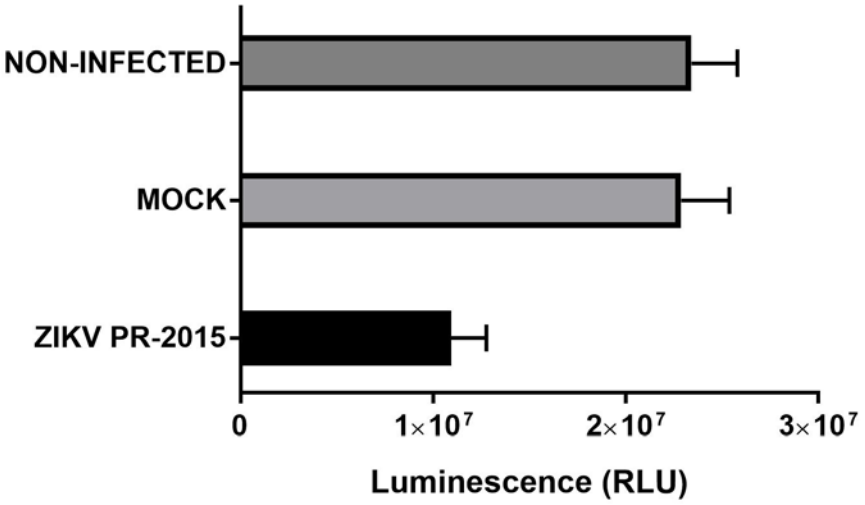

Figure 10 Exposure to ZIKV results in iDC apoptosis (As determined by Cell Titer-Glo / ATP metabolic activity)

Monocytes from two donors differentiated into iDC. iDC harvested on day 5 and left non-infected, mock-infected, or infected with ZIKV PR-2015. 48hr PI, Cell-Titer GLO luminescent cell viability assay performed on 100,000 cells per well. Read out performed on a Luminometer using manufacturer's recommended settings. Results shown in luminescence, relative light units. Averages of across both donors and error bars representing mean standard deviation.

5.1.9 Exposure of iDC to ZIKV induces TNF-α

Next, a human cytokine panel was used to measure cytokine responses in iDC to ZIKV. IFN-γ, IL-1β, IL-2, IL-4, IL-5, IL-8, IL-10, IL-13, IFN-α and TNF-α were analyzed in tissue culture supernatants. Interestingly, the only analyte in the selected panel that was shown to be increased in the ZIKV-exposed cultures was TNF-α.

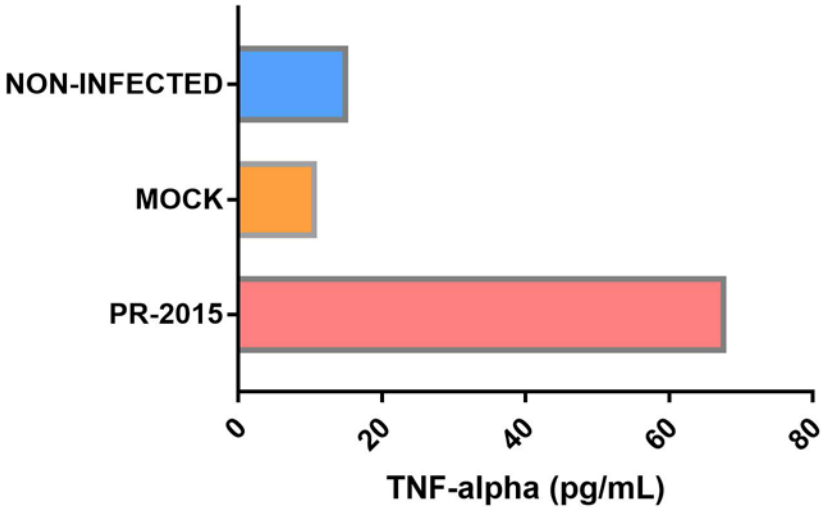

Figure 11 ZIKV induces TNF-α

iDC harvested on day 5 and left non-infected, mock-infected, or infected with PR-2015 at MOI 1. Cells stained for Flavivirus viral E protein at 48hr PI to confirm infection (data not shown). 48hrs PI culture supernatants collected. MSD multiplex cytokine array system used to detect a panel of cytokines as outlined in manufacture protocols--IL-12p70, IL-L13, IL-1b, IL-2, IL-5, TNF-α. TNF-α was the only analyte to show a difference between controls and infected samples.

5.1.10 Environmental instruction programs DC resistance or susceptibility to ZIKV infection

Next, ZIKV infection in polarized DC types was explored. In figures 6 and 7, the larger cell populations showed higher levels of infection and were more mature. By maturing cells first, followed by infection, we attempt to determine if ZIKV is preferentially infecting a matured cell or if ZIKV is driving their maturation. 5 DC types with different polarization status were examined - iDC, DC0, DC1, DC2, aDC1*. Interestingly, aDC1 showed no infection while DC2 displayed the highest rates of infection (Figure 12). DC1 showed 20% infection, DC0 50%, and iDC control infected at about 38%.

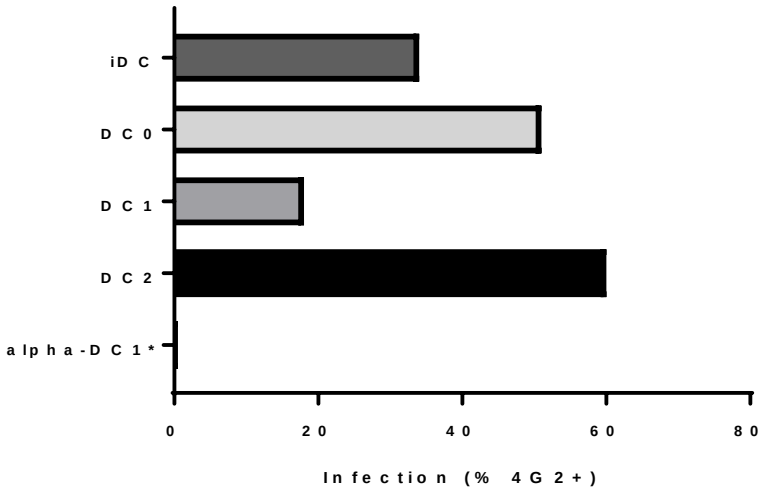

Figure 12 Mature type-2 polarized DCs are most susceptible to ZIKV infection

iDC were left alone as a control or matured by different maturing/polarization factors. DCs were harvested and infected with ZIKV PR-2015, left non-infected, or mock infected at 24hrs post maturation (only infected samples shown). Cells stained for Flavivirus viral E protein 48hrs PI and analyzed using flow cytometry.

5.2 AIM 2.A

5.2.1 CD40L functions – Critical T CD4$^+$ T helper factor

- Induces DC maturation (Figure 13A)
- Enhances DC survival (Figure 14A)
- Promotes IL-12p70 production (Signal 3)
- Supports CTL induction and survival
- Promotes intercellular trafficking (Figure 13)
    - Induces DC to DC transfer via TNT networks / DC ‘reticulation’ (30) (Figure 13B)
    - Induces DC to T cell transfer (Figure 13D)

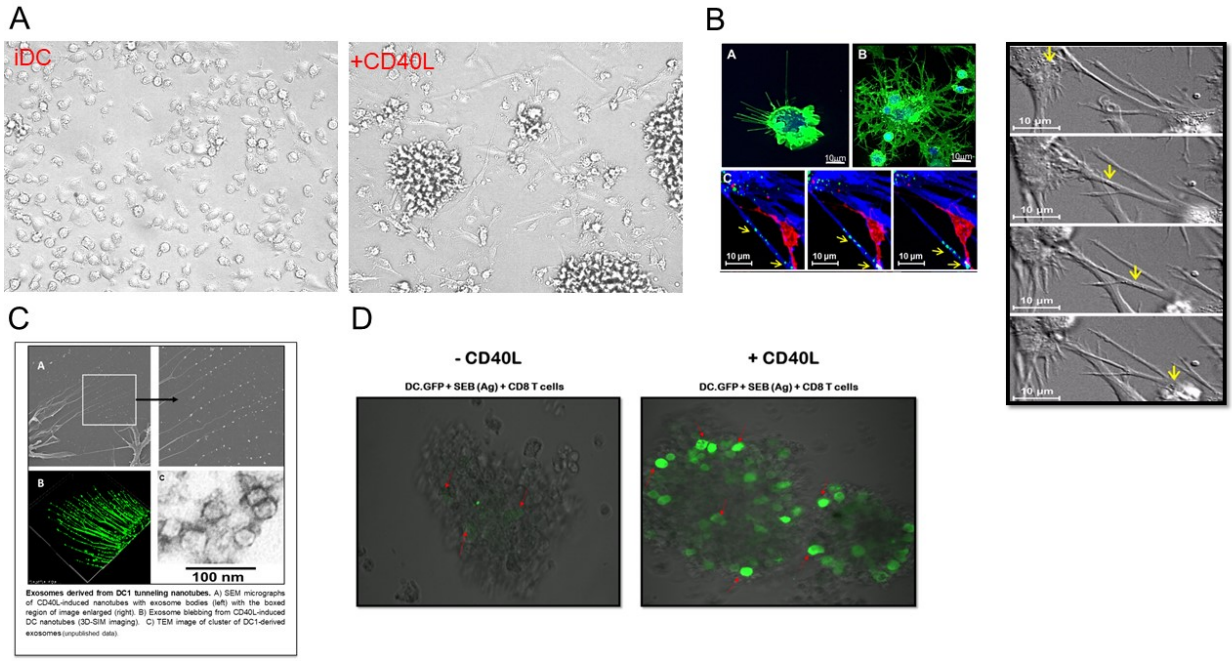

Figure 13 CD40L impact on DCs

Figure (A) iDC alone and DC stimulated with CD40L in vitro showing a mature/activated DC phenotype in culture. Figure (B) Work previously published in our lab that CD40L induces functional tunneling nanotube networks in DC1 Figure "Sequential frames of high resolution, time lapse DIC imaging (600×) of live 8 h rhCD40L- stimulated DC1 showing endogenous cell structures resembling vesicles (arrows) trafficking between neighboring cells through CD40L-induced TNTs" (28). Figure (C) Exosomes from tunneling nanotubes (unpublished data). Figure (D) CD40L found to have a significant role transfer of GFP to $CD8^+$ T cells. $CD8^+$ T cells following 4-day co-culture with DC1.GFP alone (D left) or with CD40L (D right). The red arrows = $CD8^+$ T cells expressing GFP (green).

5.2.2 T cell "help" enhances survival of ZIKV infected DC

Knowing CD40L can enhance survival of DCs (Figure 14A), we stimulated ZIKV infected DCs with CD40L and observed their survival compared to unstimulated infected cells. CD40L increased the overall survival of DC exposed to ZIKV (Figure 14B). Cell was viability further examined using Cell-Titer GLO luminescent cell viability assay quantitating cellular ATP levels present in cultures. Infected DC stimulated by CD40L had reduced change in overall metabolic activity from T=0 to T=120 compared to the controls (Figure 15).

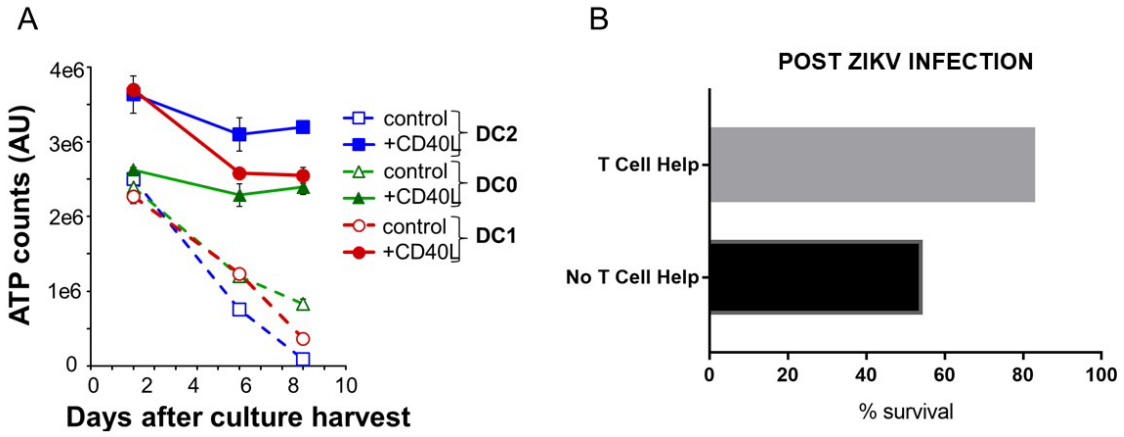

Figure 14 T cell "help" enhances survival of ZIKV infected DC

Figure (A) ATP counts in different polarized DC subtypes with and without CD40L stimulation over time (unpublished Mailliard et al). Figure (B) iDC were harvested on day 5 and infected with ZIKV PR-2015 and cultured with or with subsequent CD40L stimulation. Cells were assessed by flow cytometry for intracellular expression of the Flavivirus viral E protein at 48hrs post infection. Percent survival depicted based on FSC x SSC analysis. FSC low=apoptotic, FSC high=cells surviving.

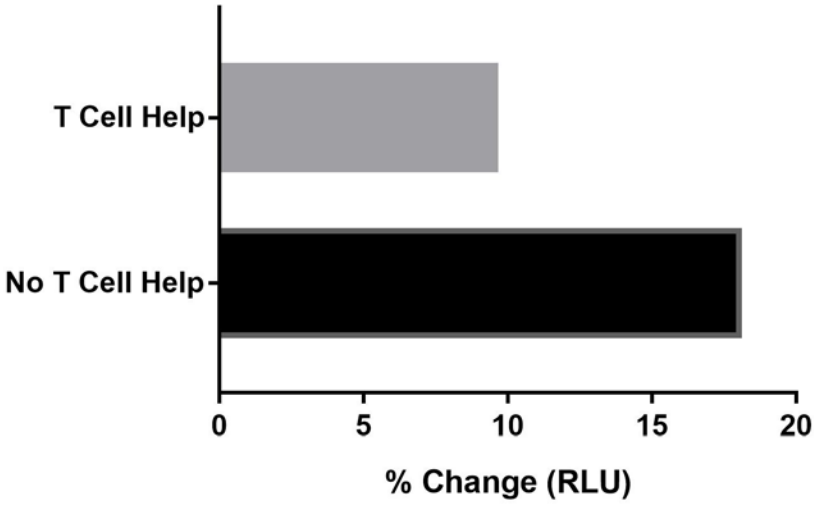

Figure 15 T Cell 'help' limits apoptosis in ZIKV exposed DC (Cell Titer-glo / ATP - metabolic activity)

iDC harvested on day 5 and left non-infected, mock-infected, or infected with PR-2015 (only infected samples shown). Cells stimulated with CD40L or left unstimulated. At time 0 and 120 hours post infection Cell-Titer GLO luminescent cell viability assay performed on 100,000 cells per well. Read out performed on Luminometer using manufacture recommended settings. Results a function of luminescence (RLU) percent change from Time 0hr to time 120hrs.

5.2.3 In-vitro DC transfer of ZIKV to bystander cells

We next explored if DC had the capacity to transfer infectious virus to other cell types and if CD40L could enhance the transfer of virus to other cell types. A co-culture of infected DCs with K562-DC-SIGN cells showed that DC can transfer infection to K562-DC-SIGN cells. CD40L stimulated cultures appeared to have comparable rates of infection to non-stimulated.

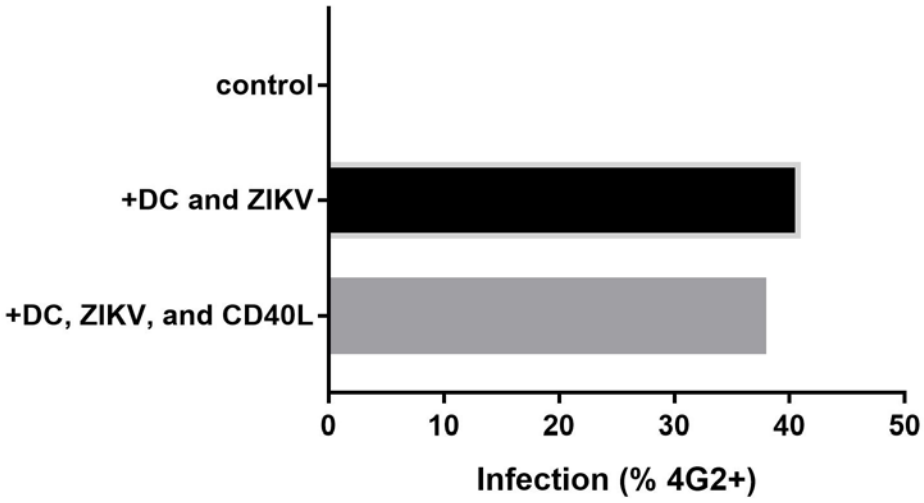

Figure 16 In-vitro DC transfer of ZIKV infection to bystander cells is not CD40L dependent

iDC and polarized DC2 (DC2 conditions shown) harvested on day 6 and left non-infected, mock-infected, or infected with ZIKV PR-2015. DCs set into culture for 24 hours. After 24 hours, K562 (overexpressing DC-SIGN) added to form co-culture at 1:2 K562:DC. Conditions stimulated with CD40L or left unstimulated. Control (DC and K562 mock), K562 +DC and ZIKV, K562 +DC ZIKV + CD40L. Bystander infection (gated on HLA negative, not shown) in K562 from co-culture shown.

5.2.4 Transfer of ZIKV is non-contact dependent.

To determine if the transfer of ZIKV to K562 cells was contact dependent, a transwell assay was performed were ZIKV infected DC were placed in the top chamber and uninfected, target K562-DC-SIGN were placed in the lower wells. Infection was detected in K562 in the lower wells of the transwell after 48hrs, indicating non-contact dependent transfer of virus from infected DC to K562. Stimulation with CD40L had minimal impact on non-contact dependent transfer.

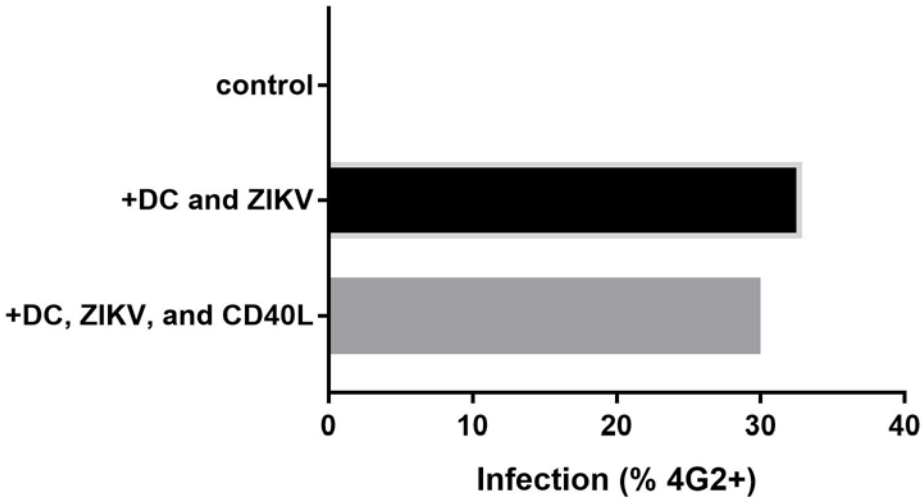

Figure 17 *In vitro* DC transfer of ZIKV infection is non-contact dependent and not impacted by CD40L

iDC and polarized DC2 (DC2 conditions shown) harvested on day 6 and left non-infected, mock-infected, or infected with PR-2015. DCs added to upper compartment of 0.4µm pore Transwell insert (Corning Life Sciences). K562 (overexpressing DC-SIGN) added to lower compartment of 24-well plate. DCs stimulated with CD40L or left unstimulated. Control (DC and K562 mock), K562 +DC and ZIKV, K562 +DC ZIKV + CD40L. K562 infection percentage shown.

5.2.5 Infection of iDC with ZIKV does not result in direct IL-12 production

The capacity of iDC infected with ZIKV to produce IL-12p70 was assessed. While Il-12p70 production was not directly induced by the ZIKV exposure (also described in Figure 12), iDC that were infected did show an enhanced responsiveness to subsequent stimulation with the T helper cell associated signal CD40L as determined by their enhanced capacity to produce IL-12p70 (Figure 17).

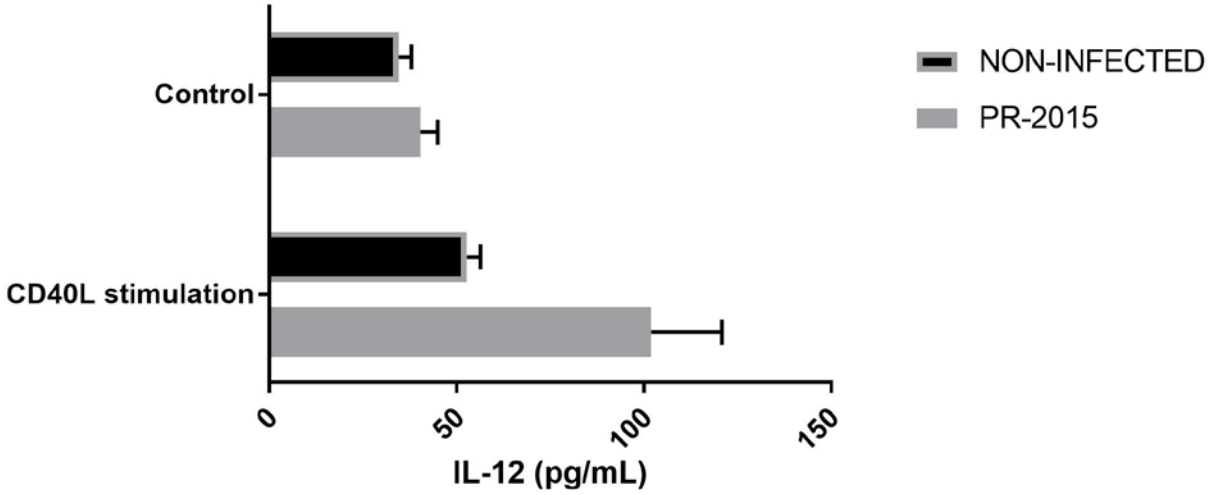

Figure 18 ZIKV infection of iDC results in an increased capacity to produce IL-12p70 following CD40L stimulation

iDC harvested on day 5 and left non-infected or infected with ZIKV PR-2015. 48hrs PI, cells harvested and stimulated with CD40L using J558 cells or not stimulated. 24 hours post stimulation, supernatants collected and IL-12p70 ELISA performed. Error bars indicate mean standard deviation.

5.3 AIM 2.B

5.3.1 DC activation by cross-reactive dengue effector memory T cells

DENV seropositive donor DC and PBL were co-cultured in the presence of either DENV NS3 peptide or ZIKV NS3 peptide. On 4th day of co-culture, microscope images of cultures were taken, and DC phenotype compared (Figure 19). Differences in the phenotypes between DC presenting either DENV or ZIKV antigen are observed. Where ZIKV antigen was presented, the DC showed possible signs of activation via elongation and adherence of the DC to plastic (Figure 19C).

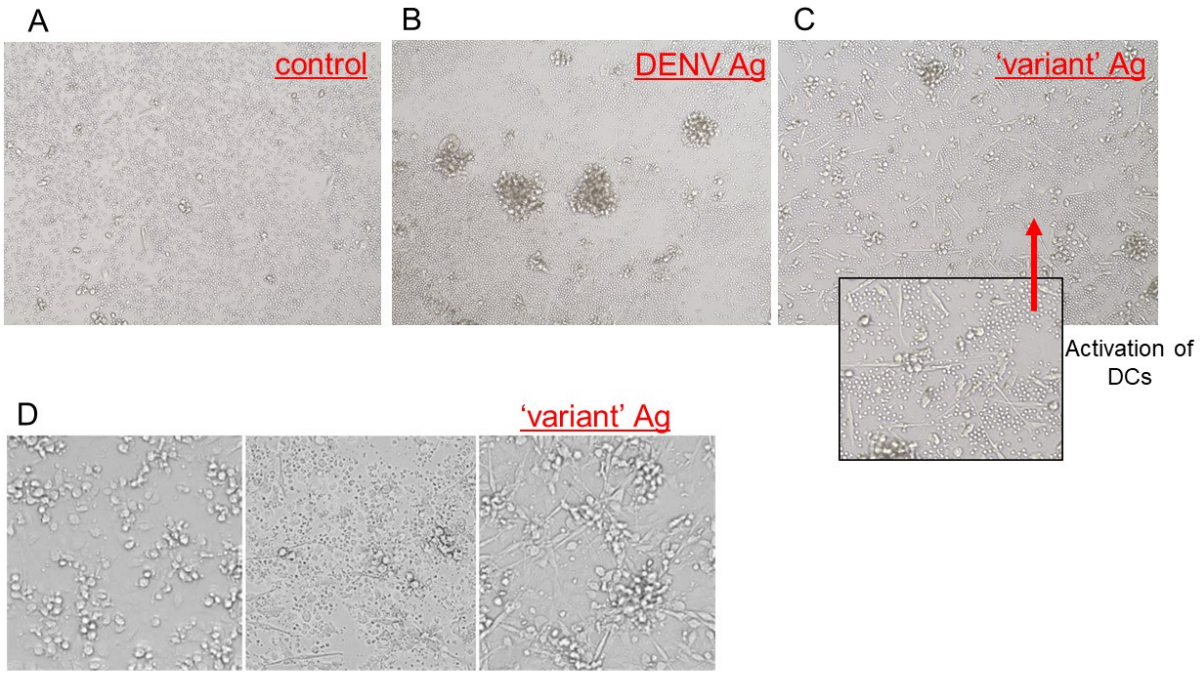

Figure 19 Evidence of DC activation by ZIKA cross reactive dengue memory T cells in co-culture

Preliminary observations **(A)** Light microscopy of αDC1:PBL coculture using DENV seropositive donor. **(B)** Light microscopy of αDC1:PBL coculture using DENV seropositive donor. Pulsed with DENV NS3 peptide pool. **(C)** Light microscopy of αDC1:PBL coculture using ZIKV seropositive donor. No antigen stimulation. Magnification 10x. (all images obtained on day 4 of coculture) **(D)** Dysfunctional killing capacity of variant peptide stimulated cross-reactive CLT. Images previously published by Mailliard et al. 2013 (26). Dysfunctional killing capacity of variant peptide stimulated cross-reactive CLT. Cellular debris in the priming peptide culture indicates a massive degree CTL-induced DC death while the elongated adherent cells in the peptide variant culture suggest cross-reactive CTL dependent DC activation.

5.3.2 DC antigen presentation is required to unveil cross-reactive T cell responses to ZIKV antigen

To further explore cross-reactivity, T cells from DENV seropositive donors were expanded in co-culture. Cross-reactive responses were then analyzed using IFN-γ ELISPOT. DENV memory responses to DENV antigen were detectable without DC present, but DC presentation was

required for sufficient detection of the cross-reactive T cell response to ZIKV antigen (Figure 20).

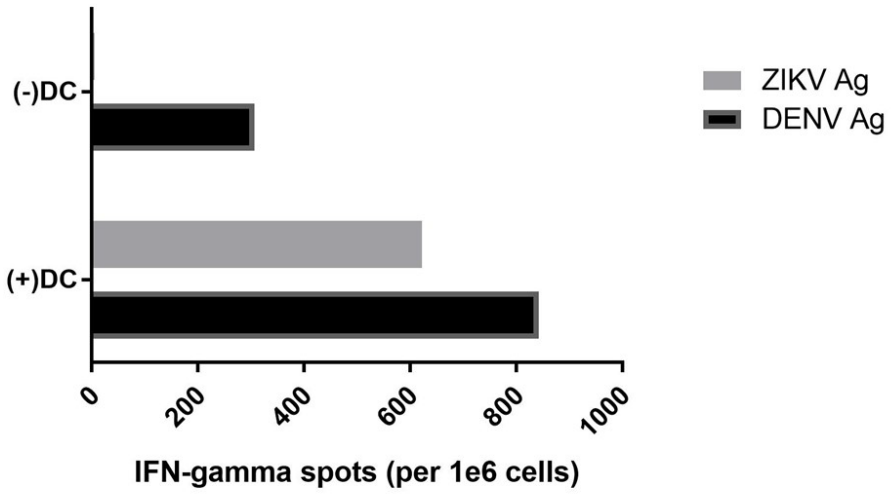

Figure 20 DC presenting ZIKV antigen are required for sufficient detection of cross-reactive T cell responses

Results from IFN-γ ELISpot. Memory T Cells originally primed by DENV Ag *in vivo* were re-stimulated and expanded *in vitro* with DENV peptide. Readout and IFN-γ performed using DENV Ag, ZIKV Ag, or no antigen in wells of ELISpot plate, with or without DC antigen presentation. Average number of spots for each condition normalized to control (no antigen) to eliminate background. Total IFN-γ producing cells displayed per $1.0x10x^{6}$ cells.

5.3.3 Evidence of DC activation by ZIKA cross reactive dengue memory T cells

T cells were isolated directly from the blood of DENV seropositive and seronegative donors. A co-culture was established using respective donors T cells and DCs, and ZIKV NS3 peptide pool was added to the cultures. In the DENV seropositive donor, possible signs of activation via elongation and adherence of the DC to plastic is observed (Figure 21).

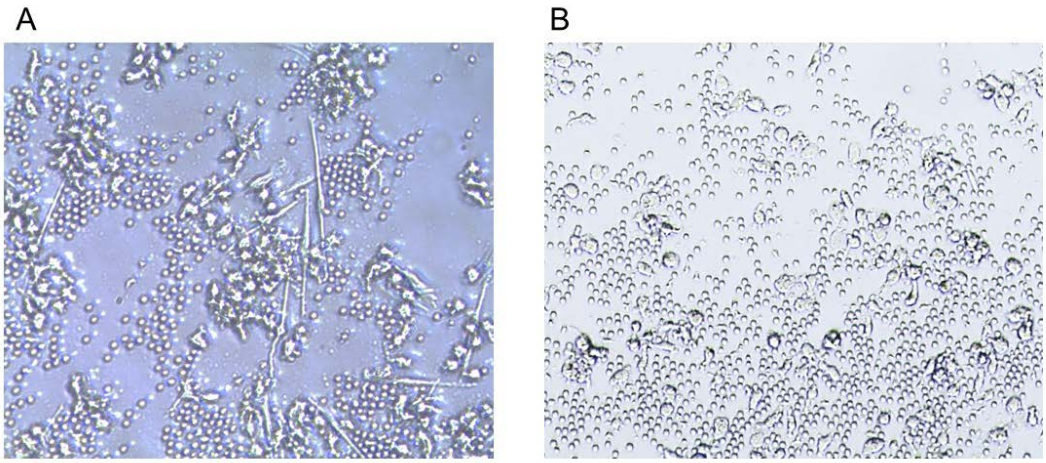

Figure 21 Cross-reactive DENV memory T cells responding to DC presenting ZIKV antigen

Immature DC presenting ZIKA peptides (15mer pool), co-cultured with T cells isolated directly from the blood of a dengue immune donors (A) (not pre-activated CTL) and confirmed seronegative donor (B).

6.0 DISCUSSION

The DC has key roles in development of immune responses and has known interactions with ZIKV. However, the nature and outcomes of this interaction, and its role in ZIKV pathology needed further elucidation. Here we hypothesized ZIKV can infect and modify the phenotype and function of dendritic cells, which influences the nature of their subsequent interplay with pre-existing ZIKV-Ag responsive memory T cells. We found that ZIKV can indeed infect both immature and mature DCs, and that DCs can transfer infection to bystander cells. We also found that exposure of DCs to ZIKV alters their function, maturation status, and survival. Interestingly, we note that the capacity of ZIKV to infect DCs is greatly influenced by the environmental signals received by DCs during their maturation process, and that type-1 polarized DC are inherently more resistant than type-2 matured DC. Importantly, when activated by the $CD4^+$ T cell helper signal CD40L, ZIKV infected DC proved to be more resistant to ZIKV-induced cell death. And finally, on the background of dengue virus immunity, we found that dengue antigen specific memory T cells can cross-react with ZIKV antigen presented by DC, leading to enhanced DC activation rather than elimination. These findings have public health significance—new details regarding ZIKV and DC interactions helps provide a better understanding of ZIKV pathogenesis overall. This work and future findings may prove pertinent for the development of effective interventions to protect and treat those who may become exposed to ZIKV.

We confirmed, as previous studies have shown, that ZIKV (both the American PR-2015 and the Asian Cambodia 2010) can infect human iDC as measured by the expression of ZIKV E protein accumulation in infected cells. Our established controls, non-infected and the mock supernatant controls, prove to be reliable negative controls as a comparison to infected cells expressing E protein at 48hr time point. To confirm that detectible E protein at the 48hr time point is not a result of virus that used at input to infect the cells, we performed a basic time course infection. Following infection of DC, 2 hours post-infection, the percent of DCs that stain positive for viral envelope protein is 0% (Figure 2A), confirming the infection detectible at 48 hours is in fact the result of DCs producing viral E protein, which accumulates in the cells. When we extend the time point out an additional several days, detectible E protein drops off in infected DC samples. Additional groups have showed a similar decline in percent cells positive for E protein following the 48 hour time point (18). The method used to infect DC and detect infection, while reliable along with the established controls, presented several challenges. Run to run infection rate variation was frequently observed using same methods, cell type, donor, and even between different batch preparations of the virus. Using the same batch and MOI of virus, differences in expression of viral E protein at 48 hours can be observed across different donors (Figure 2A). These findings align with those of Bowen et al. 2017, who further showed that this is not a function of differences in affinity for viral proteins, viral binding, differences in viral kinetics, or viral RNA synthesis (18). They proposed that it is likely due to differences in complex systems of genetics, metabolism, ER stress, and redox states between donors (18). Based on our findings that ZIKV altered the metabolic state of infected DC (Figure 10), it is plausible this could be a contributing factor to differences in viral replication. But the observed loss of metabolic activity between control and infected samples between donors did not

necessarily correlate with differences in infection rate. Larger sample size could be used to rule out metabolic differences contributing to differences in viral replication. Additionally, we showed that ZIKV can cause oxidation of cardiolipin within the mitochondrial membrane, as a function of loss of ability to retain NAO probe (Figure 9). It may be plausible that differences in viral replication could be contributed to redox state differences that develop in infected cells in response to ZIKV infection, but we would need to explore this in additional donors.

We observed a potent restriction of viral replication in ZIKV iDC receiving treatment with type I IFN, IFN-α, compared to iDC receiving no treatment. This finding appears to contradict, reports that type I interferon only modestly, non-significantly decreased ZIKV replication in DCs (18). Our conflicting result could be due to study design variation. In our experiment we used IFN-α, but the conflicting result was obtained using another type I IFN, IFN-β. Interestingly these IFNs utilize the same receptor, IFNAR. While they use the same receptor, IFN-α and IFN-β do exhibit different biological properties (31). It was also found that IFN-β, but not IFN-α, interaction with the IFNR1 receptor subunit alone, is sufficient for the generation of signals that can control transcription of a group of genes independently of STAT1 phosphorylation (32). This unique action of IFN-β could further contradict Bowen, 2016, but also questions why in our findings, IFN-α is restricting replication despite additional reports indicating ZIKV interference with STAT1 phosphorylation (18). Overall, studies observing type I IFNs impact on ZIKV replication in DC need to be expanded in much greater detail. The consensus based on published literature, is that ZIKV subverts type I IFN signaling and type I IFN responses are critical for inducing the antiviral response to flavivirus infection (2). If IFN genes are systematically downregulated, translation is inhibited, or IFN signaling is impaired, this may influence intrinsic antiviral activity, and the priming of adaptive responses. In fact,

ZIKV is found to directly antagonize type I IFN translation (18). Aligning with this report we find in iDC infected with ZIKV Type I IFN secretion was not induced by ZIKV in DCs (Figure 12). It is possible that minimal levels of IFN-α are being produced and our failure to detect IFN-α in the supernatant of infected DC is a result of an autocrine uptake of the minimal amount of IFN-α being produced. Ideally, we could block the IFNAR receptor to eliminate any autocrine uptake of cytokine to detect if any secretion is occurring, but it seems unlikely since ZIKV is likely directly inhibiting translation of type I IFNs.

Bowen et al., 2017 reported minimal upregulation of T cell co-stimulatory molecules and MHC molecules in *in vitro* infection, while Sun et al. 2017 reports co-stimulatory molecules and activation markers were downregulated in *in vitro* infection (18, 19). These differences highlighted our need to further clarify how ZIKV directly impacts the maturation phenotype of DCs. We find when comparing total DC populations maturation associated protein markers between ZIKV exposed iDC and control iDC that CD80, CD86, and HLA-DR are all modestly up-regulated (Figure 4), aligning with Bowen et al., 2017.

While we found an overall maturation of total DCs, we unexpectedly observed what we hypothesized to be a large degree of cell death occurring upon exposure iDC to ZIKV PR-2015 compared to uninfected and mock infected controls (Figure 5). ZIKV exposed cultures indicated a distinct shift to low FSC, indicating the shrinking size of the DCs. Mean size, as a component of FSC, was found to be about 20% lower in ZIKV exposed cultures across several donors at 48hr post infection. We initially speculated this is due to the shrinking and possible blebbing of DCs, which are typical characteristics of cells that undergo apoptosis leading us to ask if ZIKV is inducing apoptosis in our DCs. This prompted to explore the possibility of cell death further and additionally to analyze the distinct populations of FSC-high (larger) vs FSC-low (smaller) DCs.

The cells we expected are surviving (FSC-high) show higher levels of measurable viral E protein compared to the suspected dying (FSC-low) population (Figure 6). If the observed loss in size is cell death, it may be occurring immediately before productive infection, or via another mechanism such as bystander killing. Moreover, when we analyzed the phenotype of the distinct populations of DCs (FSC-low and FSC-high), the DC that we suspected were viable (FSC-high), appeared to have a slightly mature phenotype compared to control iDC (Figure 7). A limitation of this finding is that these results were drawn using viral E protein and surfaces stains in separate test tubes which did not allow us to visualize directly the phenotype of infected cells. Using new reagents that allowed us to observe our maturation associated protein markers and infection of DCs simultaneously, it appears that in fact that the infected cells have small upticks in expression of markers CD86, CD80, and HLA-DR (note: conclusion drawn from a very small sample cell population and need to be confirm using a larger sample of cells). Unfortunately, we attempted to repeat this process using two separate staining methods to allow us to directly visualize the surface phenotype of infected cells but were limited by the efficacy to detect infected cells with the new reagents/methods.

These findings brought about new questions we hoped to explore:

1. Is ZIKV selectively infecting a subset of more mature DC?
1. Does ZIKV infection induce maturation on a subset of DC?
2. Is ZIKV induced shrinking of DCs indicative of cell death?

It may appear that ZIKV might not necessarily be targeting matured DC and the observed maturation phenotype in the larger, more infected cells is a result of ZIKV driving their maturation. But interestingly, as we show in (Figure 12) mature cells can be targeted for infection. Because we infected an immature DC subset as well as matured DC, it seems plausible that ZIKV can in fact drive the maturation of an iDC as well as infect matured cells. Whether or not ZIKV has a preference as to which pathway (maturation being the end point) occurs remains an elusive question.

To assess if the observed morphologic changes in DC are linked to cell death we infected DC and assed their viability using live dead labeling. Baseline viability of DC infected at lower MOIs was roughly 80% and comparable to the non-infected control viability (Figure 8B). There are draw backs to using amine binding dies to assess cell death, especially apoptosis. The method detects cells with compromised membranes by reacting with free amines whether they are present on the cell surface or inside the cell. While this can detect dead cells, in apoptosis for example, cell death can occur in phases. Disrupted membranes, detectible using this dye, might not necessarily be detectible if a cell is in early stages of cell death / in the process of cell death. As a proof of principle, we exposed iDC to UV radiation, which is known to induce apoptosis in cells and analyzed their size using flow cytometry and compared their scatter plots to those where we suspected cell death due to exposure to ZIKV. In fact, the UV treated cells display a shift to low FSC (Figure 8A), comparable to the pattern observed in our DC exposed to ZIKV. This is not proof that apoptosis is occurring in our ZIKV exposed cultures so further methods were required to explore apoptosis.

Next, we infected DCs and stained them using 10-N-nonyl acridine orange (NAO). The structure and integrity of mitochondria can be assessed using NAO (33). NAO accumulates in

mitochondria and subsequently will bind mitochondrial cardiolipin (13, 33). NAO binding involves the arrangement and orientation of the cardiolipin inside the membrane (13). When reactive oxygen species production is increased, cardiolipin becomes oxidized is rearranged (13). This leads to reduced NAO-binding ability by the mitochondrial membrane (13). In fact, the rearrangement of cardiolipin is a very early stage apoptotic event, which even proceeds cytochrome C dissociations (34). Here we showed that DC exposed to ZIKV had reduced NAO-binding capacity (Figure 9A) compared to control groups, indicating early stage apoptosis in our ZIKV exposed DC. To expand on the link between cell death and shrinking in our ZIKV exposed groups, we compared the size of apoptotic cells to non-apoptotic cells based on NAO staining. The non-apoptotic cells (retaining NAO in the mitochondrial membrane) are larger while apoptotic cells are smaller (Figure 9B). This further reinforces our observation that shrinking cells are in fact apoptotic. Lastly, we explored cell viability by measuring the metabolic activity via quantification of ATP levels in DCs. In multiple donors, DCs exposed to ZIKV have significantly reduced levels of ATP (Figure 10), indicating reduced viability. We uniquely show ZIKV is causing apoptosis in iDC. If ZIKV can induce apoptosis in DCs, we must ask, would this be a beneficial outcome in a natural setting? Cell death could be a means to limit viral persistence upon infection. We hypothesize that this may be a defense mechanism of the DC, to limit spread and infection in a natural setting.

We observed a limited direct impact on DC production of cytokines induced by ZIKV (Figure 12). Interestingly, TNF-α production by iDC was induced by ZIKV infection. It is unclear if the concentration of TNF-α measured accurately reflects the full impact on TNF-α production by DC, in that we know iDC will rapidly deplete the local environment of TNF-α following its production. Autocrine TNF-α signaling will result in maturation of the DC and

blocking TNF-α can inhibit maturation. Because we earlier showed moderate signs of DC maturation, it is conceivable that the iDC are utilizing the TNF-α in an autocrine manner. These findings of minimal secretion of cytokines induced by ZIKV (other than TNF-α), aligns with other groups who explored additional cytokines not assessed here (18).

We uniquely showed that DC maturation/polarization status greatly influences their infection capacity (Figure 12). DC2 were the most susceptible polarized cell type, showing higher infection rates compared to DC0 and even iDC. Interestingly, the polarized aDC1 showed no infection what so ever, while a polarized DC1 showed low levels of infection with ZIKV (Figure 12). Whether the apparent differences of infection in these subtypes of DC is a result of differences in binding or some other cellular mechanism remains unexplored. For example, αDC1 are more suited to antigen processing and secret higher levels of IL-12 compared to PGE polarized DC2 (35). We hypothesize that this could have bigger implications in ZIKV pathogenesis overall. The correct environmental ques programming DCs are critical in achieving the desired cellular immune mechanism. It is even possible that a skew in the distribution of the type of DC in different microenvironments, for example at the site of infection, could lead to differences in disease outcomes.

We next explored the impact of the T helper signal CD40L on the survival of ZIKV infected DC. We have shown in preliminary studies that CD40L activation of differentially matured DC types extends DC *in vitro* lifespan dramatically (Figure 14). To merge the concepts of enhanced survival of DC with the fact that DC are productively infected with ZIKV, we want to assess if surrogate T helper cell signal CD40L will extend the lifespan of the infected DC. We hypothesized CD40L stimulation may result in the enhanced dissemination of viral infection to other cell types, based on our knowledge of CD40L acts as a mediator of DC intercellular

transfer. We have shown as a proof of principle that CD40L can dramatically induce both tunneling nanotube formations (30) and the release of exosomes containing cellular material (data not shown, but demonstrated using GFP as a protein marker), both processes that can result in the spread of cellular material, including infectious virus (36) to other cells.

Interestingly, exposing the DC to a surrogate memory T helper cell signal CD40L either during or following ZIKV exposure, we noted an increase in the overall survival of the DC (Figure 14). This suggests that under the right conditions, memory T cells could prolong infection in these cells. We showed CD40L minimized the decline in metabolic activity caused by ZIKV in infected DC (Figure 15), and we suspect CD40L is preventing apoptosis in general in infected DCs. To achieve a more complete picture, we want to use additional methods to assess CD40L ability to limit apoptosis in ZIKV infected DCs.

To address the concept that CD40L can mediate DC transfer of ZIKV to neighboring cell types, we infected DC2 and iDC subtypes and co-cultured respectively with K562 cells, overexpressing DC-SIGN, followed by stimulation with or without CD40L. K562 cells are an immortalised myelogenous leukemia cell line. For our purposes, these cells are transfected with a construct that overexpresses DC-SIGN, which ZIKV uses as an attachment factor for binding to the cell surface. We confirmed that K562-DC-SIGN can efficiently be infected with the PR-2015 strain of ZIKV (data not shown) Interestingly, DC2 and iDC can both pass ZIKV to K562 cell in co-culture, independently of CD40L stimulation (Figure 16), leading to productive infection in K562 cells. We suspect it is highly likely that DC would have the capacity to transfer ZIKV to additional neighboring cell types which are known to support ZIKV infection, including other DC subtypes, macrophages, Hofbauer cells, and neuronal cells—all of which may be implicated in ZIKV pathogenesis. Despite the transfer of virus to K562 independently of CD40L

stimulation, we wanted to further explore if this transfer was contact dependent, and if so, if CD40L has the capacity to drive enhanced non-contact dependent transfer of virus. Using transwells, we showed iDC and DC2 can both transfer ZIKV to K562 cells (Figure 17) in a contact independent manner. CD40L stimulation had little impact on this non-contact dependent transfer of ZIKV to the K562 cells.

We next sought to determine if ZIKV Ag presenting DC induce cross-reactive responses from heterologous Flavivirus specific memory T cells. The existence of cross-reactive T cell responses is defined in the backdrop of pre-immunity to other Flaviviruses (WNV to DENV for example), but not directly in a DENV immune backdrop in ZIKV infection. Two possible outcomes of cross-reactive T cells could be hypothesized; this could lead to viral persistence and dissemination and contribute to enhanced disease, or a functional antigen presentation and antiviral response. There is the possibility that a cross-reactive DENV $CD4^+$ memory T cell could promote survival and persistence of ZIKV infected DCs in the context as previously described via CD40L co-stimulation. If a cross-reactive CTL population exists, how would co-stimulation and immediate release of cytokines affect ZIKV infected DCs; would they provide a cross-protective response, or could it lead to a non-lytic dysfunctional CTL response, as has been described by our lab in HIV escape Ag variants which lead to dysfunctional responses and can lead to dissemination of virus (26).

We showed DENV memory responses to DENV antigen were detectable by IFN-γ ELISPOT, but professional antigen presenting DC were required for sufficient detection of the effector cross-reactive T cell response to ZIKV antigen (Figure 18). However, use of professional antigen presentation in the readout assays resulted in a high level of background. Therefore, we realized that to carry out these studies extensively, 9mer associated peptides for T

cell to T cell antigen presentation are required to ensure a more accurate readout and detection of cross-reactive responses. Interestingly, when we observe the phenotype microscopically, of DC presenting either DENV or ZIKV antigen to T cells from a DENV seropositive donor, we observe morphologic differences. In co-cultures with DENV antigen, the DC did not appear to survive and balled up into tight T cell clusters, with debris and empty space (Figure 19B). However, when the ZIKV antigen was presented, the DC instead showed signs of activation, with elongation and adherence of the DC to plastic (Figure 19C). This may suggest that the same T cells are recognizing the DC presenting antigen and responding with a different 'effector' response. This is similar to what we have previously shown in the setting of HIV (26). A similar pattern of what appears to be ZIKV antigen cross-reactive memory T cell induced DC activation could be seen in following a 24hr co-culture with freshly isolated autologous T cells isolated from a DENV seropositive donor compared to a DENV naive individual (Figure 21).

Taken together, these preliminary results offer new hypotheses that can be further examined regarding the critical and complex role of the DC in mediating ZIKV infection. Experimentally, this can be pursued further by repeating these experiments with larger numbers of biologic replicates, and with multiple strains of ZIKV. Even further detailed understanding of how host genetics and variations in cellular mechanisms affect variation in ZIKV infected individuals is required to quantify subsequent variability in the immune responses and the significance of that variability in estimating effects on health outcomes, with specific insight into dendritic cells.

BIBLIOGRAPHY

1. Armstrong N. H, W., & Tang Q. 2017. Biological and historical overview of Zika virus. World Journal of Virology 6:1-8.
2. Quicke K. M. BJR, Johnson E. L., McDonald C. E., Ma H., O'Neal J. T., Suthar M. S. . 2016. Zika Virus Infects Human Placental Macrophages. Cell Host & Microbe 20:83-90.
3. Kim S. Y. LB, Linhardt R. J. 2017. Pathogenesis and Inhibition of Flaviviruses from a Carbohydrate Perspective. Pharmaceuticals 10:44.
4. Knipe D. HP. 2013. Fields Virology, 6th ed, vol 1, 2. Lippincott Williams & Wilkins.
5. Hamel R. DO, Wichit S., Ekchariyawat P., Neyret, A., Luplertlop N., Perera-Lecoin M., Surasombatpattana P., Talignani L., Thomas F., et al. 2015. Biology of Zika Virus Infection in Human Skin Cells. Journal of Virology 89:8880-8896.
6. Tabata T. PM, Puerta-Guardo H., Michlmayr D., Wang C., Fang-Hoover J., Pereira, L. 2016. Zika Virus Targets Different Primary Human Placental Cells Suggesting Two Routes for Vertical Transmission. Cell Host & Microbe 20:155-166.
7. Dowd K. A. DCR, Pelc R. S., Speer S. D., Smith A. R. Y., Goo L., Pierson, T. C. 2016. Broadly Neutralizing Activity of Zika Virus-Immune Sera Identifies a Single Viral Serotype. Cell Reports 16:1485-1491.
8. CDC UDoHaHS-. 2018. Vaccine Testing and the Approval Process. doi:https://www.cdc.gov/vaccines/basics/test-approve.html.
9. Calvet G.A. SFBD, and Sequeira P.C. 2016. Zika virus infection: epidemiology, clinical manifestations and diagnosis. Curr Opin Infect Dis 29.
10. Ferreira M. BA, Alexandre C., et. al. Guillain–Barré Syndrome, Acute Disseminated Encephalomyelitis and Encephalitis Associated with Zika Virus Infection in Brazil: Detection of Viral RNA and Isolation of Virus during Late Infection. The American Journal of Tropical Medicine and Hygiene 97.
11. Makhluf H. SS. 2018. Development of Zika Virus Vaccines. MDPI Vaccines 6:7.
12. Organization. PAHOWH. 2017. Zika Suspected and Confirmed Cases Reported by Countries and Territories in the Americas Cumulative Cases. PAHO Reports.
13. Ferlini C. SG. 2007. Assay for apoptosis using the mitochondrial probes, Rhodamine123 and 10-N-nonyl acridine orange. Nature Protocols 2:3111.
14. Durbin AP. 2016. Vaccine Development for Zika Virus—Timelines and Strategies. Seminars in Reproductive Medicine 34:299-304.
15. Duffy MR CT, Hancock WT, et al. 2009. Zika virus outbreak on Yap Island, Federated States of Micronesia. N Engl J Med 360:2536-2543.
16. Ferreira M. L. ea. 2017. Guillain–Barré Syndrome, Acute Disseminated Encephalomyelitis and Encephalitis Associated with Zika Virus Infection in Brazil:

Detection of Viral RNA and Isolation of Virus during Late Infection ASTMH 97:1405-1409.
17. Mlakar J. KM, Tul N., Popovic M., Polj sak-Prijatelj M., Mraz J., Kolenc M., Resman Rus K., Vesnaver Vipotnik T., Fabjan Vodu sek V., et al. 2016. Zika Virus Associated with Microcephaly. NEjM 374:954-958.
18. Bowen J. R. QKM, Maddur M. S., O'Neal J. T., McDonald C. E., Fedorova N. B., Puri V., Shabman R. S., Pulendran B., Suthar M. S. . 2017. Zika Virus Antagonizes Type I Interferon Responses during Infection of Human Dendritic Cells. PLoS Pathogens 13:e1006164.
19. Sun X, Hua S., Chen H., Rosenberg E. S., Lichterfeld M., Yuet X., et. al. 2017. Transcriptional Changes during Naturally Acquired Zika Virus Infection Render Dendritic Cells Highly Conducive to Viral Replication. Cell Reports 21:3471-3482.
20. Grant A. PSS, Tripathi S., Balasubramaniam V., Miorin L., Sourisseau M., Schwarz M.C., Sa´nchez-Seco M.P., Evans M.J., Best S.M., and Garcı´aSastre A. 2016. Zika virus targets human STAT2 to inhibit type I interferon signaling. Cell Host Microbe 19:882-890.
21. Kumar A. HS, Airo A. M., Limonta D., Mancinelli V., Branton W., Hobman T. C. . 2016. Zika virus inhibits type-I interferon production and downstream signaling. EMBO Reports 17:1766-1775.
22. Olmo I. G. CTG, Costa V. V., Alves-Silva J., Ferrari C. Z., Izidoro-Toledo T. C., Ribeiro F. M. 2017. Zika Virus Promotes Neuronal Cell Death in a Non-Cell Autonomous Manner by Triggering the Release of Neurotoxic Factors. Frontiers in Immunology 8.
23. Priyamvada L. HW, Ahmed R., Wrammert J. 2017. Humoral cross-reactivity between Zika and dengue viruses: implications for protection and pathology. Emerg Microbes Infect 6:e33.
24. Q. RLLM. 2017. CD4+ and CD8+ T-cell immunity to Dengue – lessons for the study of Zika virus. Immunology 150:146-154.
25. Selin LK CM, Brehm MA, Kim S-K, Calcagno C, Ghersi D et al. 2004. CD8 memory T cells: cross-reactivity and heterologous immunity. Semin Immunol 16:335-347.
26. Mailliard R. B. S, K. N., Fecek R. J., Rappocciolo G., Nascimento E. J. M., Marques E. T., Rinaldo, C. R. 2013. Selective induction of CTL "helper" rather than killer activity by natural epitope variants promotes DC-mediated HIV-1 dissemination. Journal of Immunology 191:2570-2580.
27. Bayer A. LNJ, Ouyang Y., Bramley J. C., Morosky S., De Azeved Marque, E. T., Coyne C. B. 2016. Type III Interferons Produced by Human Placental Trophoblasts Confer Protection Against Zika Virus Infection. Cell Host & Microbe 19:705-712.
28. Costa E. GJ, Mansuy J., Chen Q., Levy C., Cartron G., Veas F., Al-Daccak R., Izopet J., Jabrane-Ferrat N. 2016. ZIKA virus reveals broad tissue and cell tropism during the first trimester of pregnancy. Scientific Reports 6.
29. Ammerman NC, Beier-Sexton, M., & Azad, A. F. . 2008. Growth and Maintenance of Vero Cell Lines. Current Protocols in Microbiology doi:http://doi.org/10.1002/9780471729259.mca04es11.
30. Zaccard C. R. WSC, Kalinski P., Fecek R. J., Yates A. L., Salter R. D., Mailliard R. B. . 2015. CD40L induces functional tunneling nanotube networks exclusively in dendritic cells programmed by mediators of type-1 immunity. J Immunol 194:1047-1056.

31. Runkel L. PL, Lewerenz M., Monneron D., Yang C., Murti A., Pellegrini C., Goelz C., Uze´ G., Mogensen K. 1998. Differences in Activity between a and B Type I Interferons Explored by Mutational Analysis. J Biol Chem 273:8003–8008.
32. Kaur S. PL. 2013. IFN-β-specific signaling via a unique IFNAR1 interaction. Nature Immunology 14.
33. Petit J. M AM, Marie-Helene R., Raymond J. 1992. 1ON-Nonyl acridine orange interacts with cardiolipin and allows the quantification of this phospholipid in isolated mitochondria. Eur J Biochem 209:267-273.
34. Belikova N.A. VYA, Osipov A. N., Kapralov A. A., Tyurin V. A., Potapovich M. V., et. al. 2006. Peroxidase activity and structural transitions of cytochrome c bound to cardiolipin-containing membranes. Biochemistry 45:4998-5009.
35. Mailliard RB. W-KA, Cai Q., et al. 2004. a-Type-1 Polarized Dendritic Cells: A Novel Immunization Tool with Optimized CTL-inducing Activity. Cancer Research 64:5934-5937.
36. Zaccard CR WS, Ayyavoo V, Rappocciolo G, Mailliard RB, Rinaldo CR. 2017. Inducible tunneling nanotube networks in pro-inflammatory dendritic cell-mediated HIV-1 trans-infection of CD4+ T cells.